Journal of
Engineering Sciences
Faculty of Engineering
Assiut University
JES
مجلة
العلوم الهندسية
كلية الهندسة
جامعة أسيوط
journal homepage: http://jesaun.journals.ekb.eg

Multi-objective Optimal Probabilistic Planning in Distribution Systems Considering Load Growth

Received 19 October 2024; Revised 4 December 2024; Accepted 4 December 2024

Ayat Ali Saleh[1]

Abstract: Distribution network planning is critical to meet load growth and ensure the reliability of the network. the load demands of electrical distribution networks is increased gradually over time, which raises active and reactive power losses and lowers bus voltages below allowable levels. The modern power system has experienced significant structural modifications as a result of the annual expansion in load. This paper presents the operation of distribution networks with dispatch able mix of different types of distributed energy resources (DERs) units considering load growth up to planning period based on Multi Variant Differential Evolution algorithm (MVDE). The electric power system is supplied by numerous capacity resources including renewable and non-renewable power resources like photovoltaic system (PV), wind turbine system (WT), fuel cell (FC), and micro-turbine (MT). The main objectives of DERs allocation are to maximize technical, economic and environmental benefits by reducing the power losses, annual cost, and greenhouse gas. The WT, PV, MT, and FC units' capacity is increased by capacity expansion planning in the radial distributed network, which is carried out over a five-year planning horizon. A comprehensive stochastic strategy is offered for a number of uncertainties, such as load increase and output power from renewable energy sources. Two IEEE bus networks are used to illustrate the suggested method's efficacy. The optimization results based on proposed algorithm are compared with some existing algorithms.

Keywords
uncertainty effect;
Multi Variant Differential Algorithm (MVDE);
Sources of renewable energy;
Power loss reduction;
Voltage deviation; Pollutant gas emissions; Cost.

1. Introduction

According to BP Energy Outlook, the demand for power has grown dramatically on a global scale, ranging from 0.9% to 1.3%, the annual load growth is important for distributed system planning since it has caused the distribution system to add new distributed energy resources to expand its capacity [1, 2]. Renewable or nonrenewable resources, such as wind turbines (WT), solar systems (PV), micro-turbines (MT), fuel cells (FC), hydroelectric generators, and diesel generators, can be used as distributed energy units [3-5]. Globally, there has been a

[1]Electrical Engineering Department, Faculty of Energy Engineering, Aswan University, Aswan, Egypt. eng_ayat87@yahoo.com

https://doi.org/10.21608/jesaun.2024.329451.1377

recent trend toward the usage of renewable energy sources, which offer long-term economic and technical advantages. Better performance, more economy, less energy losses, and cleaner energy production are all achieved with the integration of renewable energy resources [6, 7].

Both wind and solar energy are significant and good sources of renewable energy resources, which are efficient, non-polluting, and renewable. This helps to lower global carbon dioxide emissions [8, 9]. They are effective in solving load growth problems and reducing system operation cost. Traditional passive power distribution systems become active systems when distributed energy resources (DERs) are integrated. The quality of the power supply that distribution networks provide is significantly impacted by DERs. By lowering active and reactive power losses, enhancing the node voltage profile, and lowering line loads, deciding on the ideal size and placement of distributed energy resources (DERs) is crucial to enhancing system efficiency, dependability, and power quality. When DERs are assigned incorrectly, power losses increase, which raises the system's overall cost [10]. In order to reduce power loss, voltage deviation, total harmonic distortion, operating expenses, and CO2 emissions, as well as to increase voltage stability, system reliability, and stability margin, distributed energy resources have been optimized for a number of objective functions [10].

Optimization techniques are constantly being developed to maximize the benefits of distributed energy resources. The current algorithms are primarily concerned with determining the ideal DER unit types, locations, and operating power factors. Typically, this is accomplished by creating appropriate objective functions that optimize different aspects of the distribution system, like actual and reactive power losses. Conventional methods, intelligent search methods, and hybrid heuristic approaches are the three primary groups into which optimization techniques fall. Numerous numerical techniques have been proposed in [11] to determine the optimal location and capacity of the DERs unit in the radial distribution network. It is evident that these algorithms are best suited for solving linear problems and not for nonlinear ones, and that choosing the right initial convergence value is necessary to find a global solution.

To get around the limitations of the numerical methods, many optimization strategies have been devised. The ideal size and placement of DER units in a radial distribution network have been determined in [12] using the BAT optimization technique. In [13], the best allocation of inverter-based distributed energy resources (DERs) in distribution networks were chosen using the non-dominated sorting genetic algorithm II to solve the suggested multi-objective issues. Additionally, a Monte Carlo simulation was used to address the uncertainty of the load and electricity produced by each DER using a time-series-based probabilistic technique. The primary objectives of this allocation and sizing challenge are to decrease voltage variance, short-circuit currents, and investment and operational costs.

1.1. Literature State of the Art

Sunflower optimization algorithm (SOA), salp swarm method (SSA), and enhanced coyote optimization algorithm (ECOA) have been considered used to determine the best distribution of DERs while decreasing operating cost, minimizing power loss, and improving voltage stability [14].

In [15] different algorithms have been used to study the effect of the wind turbine (WT) generator's uncertainty on radial distribution systems. The modeling of PV system components has been discussed in [16], optimization techniques used to select the best size of PV cell. Hybrid renewable energy systems based on WT and PV units has been integrated with other units like: micro turbine (MT), fuel cell (FC), biomass, and battery storage system (BSS), to increase benefits of these hybrid combinations [17, 18]. An energy storage system (ESS), heat pump, and an electric vehicle were used to maximize profits and minimize electricity charges based on multi-objective optimization problem considering residential homes [19].

The authors concentrated on analyzing the system, PV and WT uncertainty to determine the distribution of renewable energy while optimizing a hybrid WT, PV, and MG system using the multi-objective salp swarm method. [20]. Yang, M et al. [21] used Monte Carlo method to research how the generation of renewable energy is affected by uncertainty on microgrid dispatching. By using a mathematical optimization algorithm that takes into account generation and demand uncertainties, Hadi Abdulwahid et al. [22] looked into how best to operate a hybrid WT/PV system, the goals of this allocation and sizing problem are to minimize energy losses, the HS cost, and the voltage profile as well as to increase reliability in the form of the energy-not-supplied (ENS) index. One possible approach has been used to reduce carbon emissions is the multi-energy complementary integrated energy system (MCIES) [23]. To handle the optimization problem with uncertainties, the non-dominated sorting genetic algorithm-II (NSGA-II) is taken into consideration and integrated with other methods. The results show the benefits of the proposed approach over the traditional deterministic optimization approach for comprehensive economic analysis.

Nooriya A et al. [24] creates an enhanced Artificial Neural Networks (ANNs) model that uses an Adaptive Back propagation Algorithm (ABPA) to anticipate electrical load demand over the long term, following best practices. The purpose of this study is to present an Adaptive Backpropagation Algorithm (ABPA) for long-term forecasts that are more reliable and accurate. To handle the impact of accumulated errors created over extended periods of prediction, the standard Backpropagation Algorithm (BPA) algorithm's forecasting component is further improved to reach this precision. An overview of optimization approaches used to identify the most effective placement and size of DERs units in electric power systems is presented below Table 1.

Table.1 Summarizes the strategies used to allocate distributed energy resources (DERs) in

electric distribution networks.

Ref	Optimization algorithms	IEEE bus System	objective function	Renewable energy			Uncertainty effect	Load growth
				WT	PV	WT&PV		
[15]	MODA and MODE	33, and 69-bus		✓			✓	
[16]	A Review of Criteria, Constrains, Models, Techniques, and Software Tools	Different systems			✓			
[17]	adaptive weighted particle swarm optimization		MO			✓		
[18]	Mixed-Integer Linear Programming (MILP)	small Japanese island	MO			✓		
[20]	PSO and GA algorithms	33, and 69-bus	MO	✓	✓		✓	
[21]	Monte Carlo method and PSO	Different systems	MO	✓	✓		✓	
[22]	improved escaping-bird search algorithm (IEBSA)	33-bus	MO			✓	✓	
[25]	Improved Wild Horse Optimization algorithm (IWHO)	33, 69, and 119-bus	SO		✓			
[26]	An improved escaping-bird search algorithm (IEBSA)	33-bus	MO (PSM)			✓	✓	
[27]	Multi-objective Backtracking search algorithm (PMBSA)	67, and 118-bus	MO (PSM)			✓	✓	
[28]	Bee algorithm	33-bus	MO (PSM)			✓		
[29]	Multi-objective Particle swarm optimization (PSO) technique	94-bus	MO (PSM)			✓		
[30]	Art Evolutionary Algorithms (EAs)	33 and 118 bus	MO (PSM)	✓	✓			
[31]	The multi-objective salp swarm algorithm (MSSA)	33, 69, and 119	MO			✓	✓	
[32]	Artificial hummingbird algorithm (AHA)	33, and 69-bus	MO				✓	
[33]	The Equilibrium Optimizer (EO)	69, and 94-bus	MO				✓	
[34]	Bee algorithm	33-bus	MO				✓	
[35]	Mixed-integer linear programming (MILP)	Microgrid	SO	✓			✓	
[36]	ALO	33, 69, and 119	MO	✓	✓			
[37]	the dingo optimization algorithm (DOA)	33, and 62-bus	MO	✓				
[38]	PSO	34, and 69-bus	MO	✓	✓		✓	✓
[39]	MOALO	69-bus	SO	✓	✓			
*	Proposed algorithm	33, 69	MO	✓	✓	✓	✓	✓

1.2. Research Gap

According to the literature study, load growth research continues to play a major role in the electric power system, which may be having an effect on distributed network management and operation. In order to determine the best position, sizes, and operational power factor of distributed energy resource (DERs) units while taking into account the increase in load, the Multi Variant Differential Evolution Algorithm (MVDE) is introduced in this work for the simultaneous optimization of DERs penetration level and network performance index. There are three objective functions developed. These include the following: (I) pollution index, (II) DG penetration level, and (III) network performance indicator. The voltage profile is improved and network losses are decreased by minimizing the third goal. A distribution network owner (DNO) can lower the capital investment, operational, and maintenance costs of implementing DERs by minimizing the first and second goal. The suggested algorithm's optimization results are contrasted with those of a few other algorithms. A radial distribution system with IEEE 33 and 69 is used to validate the method.

1.3. Article Contribution and Organization

The following points represent the work contributions, which are:

i. An increase in load was planned for 5 years, and
ii. The amount of energy required during each year was determined.
iii. The best location of different type of DGs has been determined during each year.
iv. Impact of renewable energy resource, such as wind turbine and photovoltaic system on the performance of the network is covered.
v. New WT, PV, FC, and MT units with suitable capacity, location, and operating power factor are integrated.
vi. The optimal location and size of WT, PV, FC, and MT units is obtained by Multi Variant Differential Evolution algorithm (MVDE).
vii. Annual load growth for electrical distribution systems is covered.
viii. The technique guarantees satisfactory solution for all possible operating conditions.
ix. Single and multi-objective planning is covered.
x. The technical, economic and environmental benefits of DERs are presented.
xi. Several IEEE power systems have tested the suggested approach.
xii. The different algorithms are qualitatively compared (MVDE, WOA, and GA).
xiii. a comparison is done between proposed Algorithm and other Algorithm such as SA, EAs, GA-PSO, ABC-CSO, ABC-BAT, ALO and PSO method.
xiv. Model of Uncertainties based on PEM Method is presented.

This paper is structured as follows: Section 2 discusses the formulation of the problem, which encompasses the objective functions and the constraints of the system. Modeling of DERs is explained in section 3. Section 4 provides a comprehensive description of the Model of Uncertainties using the PEM method. The MVDE algorithm is detailed in Section 5. The results of the simulation and the discussion, which are based on standard test systems, are illustrated in Section 6. Finally, the conclusions of this work are presented in Section 7.

2. Problem Formulation

Determining the best distribution of hybrid renewable energy systems is the major goal of the suggested method for power losses, cost and emission minimization to maximize economic, technical and environmental benefits by reducing the power losses, annual cost, and greenhouse gas with satisfying the system constraints.

2. 1 Objective Function Definition

a) Power loss minimization

Fig. 1 shows a single line diagram of a radial distribution system. According to a predefined growth rate, the system's load under the impact of annual growth is proportionate to the original loads as follows [40]:

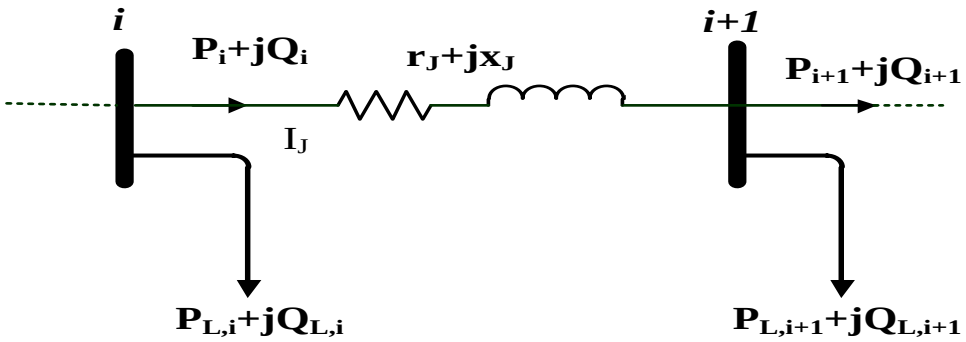

Fig 1. Single line diagram of a radial distribution system.

$$P_{Li}(y) = P_{Li}(0) \times (1+g)^{y} \quad (1)$$

$$Q_{Li}(y) = Q_{Li}(0) \times (1+g)^{y} \quad (2)$$

The following is the active and reactive power:

$$P_i = P_{i+1} + P_{Li}(y) + r_J \left(\frac{P_i^2 + jQ_i^2}{|V_i|^2}\right) \quad (3)$$

$$Q_i = Q_{i+1} + Q_{Li}(y) + x_J \left(\frac{P_i^2 + jQ_i^2}{|V_i|^2}\right) \quad (4)$$

The magnitude of the voltage is given as follows:

$$V_{i+1}^2 = V_i^2 - 2(rP_i + xQ_i) + \left(r_J^2 + x_J^2\right)\left(\frac{P_i^2 + jQ_i^2}{|V_i|^2}\right) \quad (5)$$

The following shows the active and reactive power flow after DG installation at bus i+1:

$$P_i = P_{i+1} + P_{Li}(y) + r_J \left(\frac{P_i^2 + jQ_i^2}{|V_i|^2}\right) - P_{DG} \quad (6)$$

$$Q_i = Q_{i+1} + Q_{Li}(y) + x_J \left(\frac{P_i^2 + jQ_i^2}{|V_i|^2}\right) - Q_{DG} \quad (7)$$

The active power losses can be calculated as shown:

$$P_{loss(J)} = r_J \left(\frac{P_i^2 + jQ_i^2}{|V_i|^2} \right) \quad (8)$$

The reactive power losses can be finding as shown:

$$Q_{loss(J)} = x_J \left(\frac{P_i^2 + jQ_i^2}{|V_i|^2} \right) \quad (9)$$

Reducing the voltage deviations in the following ways will enhance the voltage profile:

$$VD = \sum_{n=1}^{n_{bus}} (V_n - V_1)^2 \quad (10)$$

The following is a formulation of the generalized objective functions:

$$f = \sum_{i=1}^{nl} (P_{loss}(i)) \quad (11)$$

b) Minimization of Cost

The following is the objective function for cost minimization [41]:

$$F_{obj2} = Cost = Cost_{grid} + \sum_{i=1}^{N_{DERs}} C_{DERs,i} \quad (12)$$

$$Cost_{grid} = P_{grid}.\pi_{grid} \quad (13)$$

$$C_{DERs,i} = Cost_{DERsi}^{FX} + Cost_{DERs,i}.P_{DERs,i} \quad (14)$$

The formula below can be used to determine a fixed cost:

$$Cost_{DERs,i}^{FX} = \frac{C_{cap,i}.\ P_{cap,i}.\ rb}{T * 365 * 24 * K_{DERs,i}} \quad (15)$$

A variable cost can be calculated by:

$$Cost_{DERs,i} = C_{O\&M,i} + C_{F,i} \quad (16)$$

Where $C_{O\&M,i}$ is the DERs operation & maintenance cost, $C_{F,i}$ is the Cost of fuel for DERs. The cost of the suggested technologies is presented in Table 2.

Table.2 The cost of the suggested technologies

Generation	Capacity (kW)	Capacity Factor	Life Time (Year)	Capital Cost ($/kW)	Maintenance Cost ($/kWh)	Annual Conversion Factor
FC	400	0.4	10	3674	0.001	0.1006
MT	250	1	10	750	0.039	0.2152
PV	300	0.25	20	6675	0.005	0.0543
WT	300	0.2	20	1500	0.005	0.1006

c) Minimization of Emission

Reducing emissions from various power sources and the grid is the main aim of this project. The three most significant pollutants—carbon dioxide (CO2), nitrogen oxides (NOx), and sulfur dioxide (SO2)—are taken into account. The following is an expression for the equation used to lower emissions [42]:

$$F_{obj3} = \sum_{i=1}^{N_{MT}} E_{MTi} + \sum_{i=1}^{N_{FC}} E_{FCi} + \sum_{i=1}^{N_{WT}} E_{WTi} + \sum_{i=1}^{N_{PV}} E_{PVi} + E_{Grid} \quad (17)$$

$$E_{MTi} = (CO_2^{MT} + NO_x^{MT} + SO_2^{MT}) * P_{MTi} \quad (18)$$

$$E_{FCi} = (CO_2^{FC} + NO_x^{FC} + SO_2^{FC}) * P_{FCi} \quad (19)$$

$$E_{WTi} = (CO_2^{WT} + NO_x^{WT} + SO_2^{WT}) * P_{WTi} \quad (20)$$

$$E_{PVi} = (CO_2^{PV} + NO_x^{PV} + SO_2^{PV}) * P_{PVi} \quad (21)$$

$$E_{Grid} = \left(CO_2^{Grid} + NO_x^{Grid} + SO_2^{Grid}\right) * P_{Gridi} \quad (22)$$

The different values of the grid and the DERs parameters are listed in Table 3.

Table.3 Emission related to grid and resources

Emission type	Emission factors (lb/MW h)				
	Grid	MT	FC	WT	PV
NOX	5.06	0.4	0.03	0	0
SO2	11.6	0.008	0.006	0	0
CO2	2031	1596	1078	0	0

2. 2 Constraints

When using the optimization process to find the best DG installation, the following operating limitations in RDS must be considered:

a) Equality constraints

The constraint presents the balance between consumption side and supply side. Here, the consumption power is shown by the sum of total load power and total losses in all branches and the supply power is the sum of power generated at slack bus and power generated by all DGs, which constraint can be computed as:

$$AP_{Gr} + \sum_{k=1}^{NDG} AP_{DERs,k} = \sum_{i=1}^{k} AP_{Lo,i} + TAPL_{DERs} \quad (23)$$

$$RP_{Gr} + \sum_{k=1}^{NDG} RP_{DERs,k} = \sum_{i=1}^{k} RP_{Lo,i} + TRPL_{DERs} \quad (24)$$

b) Inequality constraints.

Bus voltage constraints: Once the ideal placement and size of DERs have been established, each bus's bus voltage should be limited as follows:

$$V_i^{min} \le V_i \le V_i^{max}, \quad i = 1, 2, \dots, N_{bus} \tag{25}$$

DERs sizing limits: The size of all the DERs shouldn't exceed the distribution network's load demand. The DERs have the following size:

$$AP_{DERs}^{min} \le AP_{DERs,k} \le AP_{DERs}^{max} \tag{26}$$
$$RP_{DERs}^{min} \le RP_{DERs,k} \le RP_{DERs}^{max}$$

DERs location limits: The location of DERs cannot be slack bus (Bus 1) and follows the inequality below:

$$2 \le \mathrm{RP_{DERs,k}} \le \mathrm{N_{bus}} \tag{27}$$

Line capacity limits: The current in some branches is increased after integrating DERs with best location and size, so the branch current must be limited as follows:

$$\mathrm{I_b} \le \mathrm{I_b^{max}} \tag{28}$$

Power factor limits: The power factor of each DG is limited to the range from 0.85 lagging to 0.99.

$$0.85 \le \mathrm{pf_{DRs,i}} \le 0.99 \tag{29}$$

3. Modeling of hybrid energy system components

The HRES employed in this study includes fuel cells (FC), wind turbines (WT), micro-turbines (MT), and photovoltaic arrays (PV).

3.1. Wind energy subsystem modeling

The wind speed determines how much electricity is produced by WT. Eq. (30) presents the formula for the electric power produced by WT [43]:

$$P_w(V_{wind}) = \begin{cases} 0 & v_{wind} < v_{ci} \quad or \; v_{co} \le v_{wind} \\ p_R.\dfrac{(v_{wind} - v_{ci})}{(v_r - v_{ci})} & v_{ci} \le v_{wind} < v_r \\ p_R & v_r \le v_{wind} < v_{co} \end{cases} \tag{30}$$

The equation of the Probability Density Function $\mathrm{f_{pw}(P_w)}$for the power generated by WES is presented in (31):

$$f_{pw}(P_w) \begin{cases} 1 - [F_v(v_{co}) - F_v(v_{ci})]p_w = 0 \\ \left(\dfrac{(v_r - v_{ci})}{p_R}\right)\left(\dfrac{\pi}{2V_m^2}\right) * \left(v_{ci} + (v_r - v_{ci}).\dfrac{p_w}{p_R}\right) * exp\left[-\left(\dfrac{v_{ci} + (v_r - v_{ci}).\dfrac{p_w}{p_R}}{\dfrac{2}{\sqrt{\pi}}V_m}\right)^2\right] \\ F_v(v_{co}) - F_v(v_r)p_w = p_R \end{cases} \tag{31}$$

3.2. Photovoltaic system modeling (PVS)

The following is a model of the behavior of solar irradiation using the Beta PDF and CDF equations [43].

$$f_B(s_i) = \begin{cases} \frac{\Gamma(\alpha+\beta)}{\Gamma(\alpha)\Gamma(\beta)} . s_i{}^{(\alpha-1)}(1-s_i)^{(\beta-1)} & for\ 0 \le s_i \le 1\ , \alpha \ge 0, \beta \ge 0 \\ 0 & otherwise \end{cases} \quad (32)$$

$$F_B(s_i) = \int_0^{si} \frac{\Gamma(\alpha+\beta)}{\Gamma(\alpha)\Gamma(\beta)} . s_i{}^{(\alpha-1)}(1-s_i)^{(\beta-1)} dsi \quad (33)$$

Eq. (34) shows the Probability Density Function f_pw (P_w) equation for the power produced by PVS.

$$f_{P_{pv}}(P_{pv}) = \begin{cases} \frac{\Gamma(\alpha+\beta)}{\Gamma(\alpha)\Gamma(\beta)} . (A_c . \eta . s_i)^{(\alpha-1)}(1-A_c . \eta . s_i)^{(\beta-1)} & if\ P_{pv} \in [0, P_{pv}(si)] \\ 0 & otherwise \end{cases} \quad (34)$$

3.3. Full Cell Unit (FC) Model

Here is the equation for the electric power produced by FC [44]:

$$C_{FC} = C_{gasFC} * \frac{P_{FC}}{\eta_{FC}} \quad (35)$$

3.4. Micro Turbine Unit (MT) Model

The following is the equation for the electric power produced by MT [44]:

$$C_{MT} = C_{gasMT} * \frac{P_{MT}}{\eta_{MT}} \quad (36)$$

4. Model of Uncertainties based on PEM Method

A convenient tool for dealing with uncertainties is Point estimate method (PEM). This method's specifics are drawn from [45–46]. The load uncertainty is represented in this study by applying (2m + 1) Hong's PEM scheme to three buses in each distribution network. To estimate the load-flow solution based on the PEM technique, the optimization methods in each case study carried out (2×3+1) load-flow calculations, taking into account three uncertain system parameters in each test system. The Point Estimate Method's general steps [6]:

Step 1: The input variables' statistical data is founded.

Step 2: Each input variable's concentration is computed.

Step 3: The weighted probability factor evaluates the F function at the positions $(p_1; p_2; \ldots; X_{1,k}; \ldots; p_{m-1}; p_m)$.

Where p_1 is the input variable's mean valueX_1. The kth location $X_{1,k}$and the mean value of m-1 remaining input variables $(p_1; p_2; \ldots; p_{l-1}; p_{l+1}; p_{m-1}; p_m)$ are included in the points $(p_1; p_2; \ldots; X_{1,k}; \ldots; p_{m-1}; p_m)$

Step 4: The output variable (Z)'s statistical data are ascertained as follows:

$$F(Z = F(p_1; p_2; \ldots; p_l; \ldots; p_m; c)) \tag{37}$$

Step 5: The mean value (μ_{pl}) and variance value (σ_{pl}) of each random variable $p_1$are calculated for the three locations.

$$p_{lk} = \mu_{pl} + \varepsilon_{lk}\sigma_{pl} \qquad k = 1, 2, 3 \tag{38}$$

Step 6: The weighting factor w_{lk} and standard location of the unknown parameters can be computed using:

$$\varepsilon_{lk} = \frac{\lambda_{13}}{2} + (-1)^{3-k}\sqrt{\lambda_{13} - \frac{3\lambda_{14}^2}{4}} \quad k = 1, 2 \;\; \varepsilon_{l3} = 0 \tag{39}$$

$$w_{lk} = \frac{(-1)^{3-k}}{\varepsilon_{lk}(\varepsilon_{l1} - \varepsilon_{l2})}, w_{l3} = \frac{1}{m} - \frac{1}{\lambda_{14} - \lambda_{13}^2} \qquad k = 1, 2 \;\; \varepsilon_{l3} = 0 \tag{40}$$

Step 7: This step will compute the F function at this moment and its new weighting factor (w_0) by:

$$w_0 = \sum_{l=1}^{m} w_{13} = 1 - \sum_{l=1}^{m} \frac{1}{\lambda_{14} - \lambda_{13}^2} \tag{41}$$

In this work, PV and WT output power are modeled under the influence of uncertainties using (K = 3, ε_{lk}= 0). Following the computation of two sets of locations and weights for every point (pl, k, ωl, k, k=1, 2), the output function for every variable and concentrated point Z(l, k), Z will be determined using $F(M_{p1}, M_{p2}, \ldots, p_{lk}, \ldots, M_{pm})$, which is computed using:

$$E(Z^J) \cong \sum_{l=1}^{m}\sum_{k=1}^{k} w_{lk} * \left[F\left(M_{p1}, \quad M_{p2}, \ldots, p_{lk}, \ldots, M_{pm}\right)\right]^j \tag{42}$$

5. Proposed Method

The proposed framework is a generalized method for finding feasible solutions to locate the DERs based on optimization algorithms

5.1. Multi-Variant Differential Evolution (MVDE) method

The optimal DERs allocation problem that was previously discussed is connected to the large-scale optimization problems. To overcome this obstacle, a successful search method is needed. One potentially helpful method for managing challenging, high-dimensional scenarios while improving search features is the Differential Evolution (DE) strategy. The DE method has been utilized as a search engine in this work due to its quick convergence, robustness, and effectiveness in identifying high-scale problems. In this regard, Multi-Variant

Differential Evolution (MVDE) is recommended as an essentially parameter-free optimization method. The main objective of the proposed approach was to prevent early convergence, reduce the probability of local optima trapping, and enhance the original DE's capability for global search.

The suggested MVDE integrates two high random scaling factors (based on logistic and cosine distributions) with five distinct mutation techniques in order to preserve population variety throughout the optimization process. The main stages of MVDE algorithm are listed below [47].

a) Initialization

In order to distribute the limited search space as widely as possible, it starts by solving the d-dimensional optimization problem using initial solutions (, initial candidate population) generated at random as follows:

$$x_{ij} = \text{rand}[0,1] \cdot \left(x_j^{max} - x_j^{min}\right) + x_j^{min} \quad \forall\ i \in \{1,2,\dots,NP\};\ \ j \in \{1,2,\dots,d\} \tag{43}$$

b) Proposed distributions

The two parametric distributions with completely distinguishable tail thicknesses are the logistic and cosine distributions. Based on the advancement of optimization operations, the probability of choosing each random generator is proposed.

F is highly likely to have developed in the first generations, according to the cosine distribution. The logistic distribution is more likely to be used at the end of optimization, though. These two distributions are so used.

c) Crossover

A crossover is suggested in order to broaden the variety of the perturbed variable factors. In the end, the crossover probability constant is selected to rise linearly from zero to 0.5 iterations using the subsequent formula:

$$\text{CR} = g/(2G)\ (\text{x}) \tag{44}$$

The following is a presentation of the binary crossover mapping matrix A of dimension n×d:

$$A_{ij} = Ind_{\ ij} \geq CR \tag{45}$$

The 0-1 matrix A is used for mapping the above-mentioned continuous scaling factor as follows;

$$F_{ij} = A_{ij}.* F_{ij} \tag{46}$$

d) Selection

Based on the adaptive crossover rate, the following criteria are used to choose the qualified parents of size N_p from the top-ranked solutions:

$$N_p = n * (1 - CR) \tag{47}$$

The main steps of MVDE algorithm are listed below

1. Establish the population number NPop (k=1….NPop), the number of decision variables

D (j=1….D), the higher MaxVar and lower MinVar boundaries of the decision variables, and the maximum number of iterations MaxIt(i=1…. MaxIt).

2. For every population member, choose the starting values of the position vector u_k and the associated objective function OF_k
3. Compute the optimal values of the objective function (OF_k^{best}) and the position (u_k^{best}) for i = 1
4. For ($i = 2;\ i++; i \leq MaxIt$) do, use (x) to Compute the crossover factor CR
5. For ($k = 2;\ k++; k \leq NPop$) do, if ($rnd > 3 * CR$), Use the cosine distribution to calculate the self-adaptive scaling factor $[SF]_{k,D}$. Use the logistic distribution to calculate the self-adaptive scaling factor $[SF]_{k,D}$ as follow:

$$[SF]_{k,D} = \begin{cases} \frac{2}{\pi} sin^{-1}\left(2 * [rand]_{k,D} - 1\right), cosine\ distributio \\ [rand]_{k,D} - 0.1 * \log\left(\frac{1}{[rand]_{k,D}} - 1\right), logistic\ distribution \end{cases} \quad (48)$$

6. Calculate the binary matrix by utilizing:

$$[B]_{k,D} = [rand]_{k,D} > CR \quad (49)$$

7. use the equation for the self-adaptive scaling factor [SF]k,D:

$$[SF]_{k,D} = [B]_{k,D} > [SF]_{k,D} \quad (50)$$

8. In each iteration, determine the parent selection using:

$$NPop^p = k * 1 - CR) \quad (51)$$

9. Calculate the location
   - If (i $< 0.2 *$ MaxIt)

$$\mathrm{x_{ig}} = \mathrm{x^i_{r1g}} + \mathrm{F.\,(x^i_{r2g}} - x^i_{r3g}) + F.\,(x^i_{r4g} - x^i_{r5g});\ \text{//DE/rand/2} \quad (52)$$

   - If (t $< 0.4 *$ MaxIt)

$$\mathrm{x_{ig}} = \mathrm{x^i_{r1g}} + \mathrm{F.\,(x^i_{r2g}} - x^i_{r3g});\ \text{/DE/rand/1} \quad (53)$$

   - If (t $< 0.6 *$ MaxIt)

$$\mathrm{x}_{ig} = x_{ig} + F.\left(x_{best.g} - x_{ig}\right) + F(x^i_{r2g} - x^i_{r3g});\ \text{//DE/target-to-best/1} \quad (54)$$

   - If (t $< 0.8 *$ MaxIt)

$$\mathrm{x}_{ig} = x_{best,g} + F(x^i_{r1g} - x^i_{r2g}) + F(x^i_{r3g} - x^i_{r4g});\ \text{//DE/ best/2} \quad (55)$$

   - Else

$$\mathrm{x}_{ig} = x_{best,g} + F(x^i_{r1g} - x^i_{r2g};\ \text{//DE/ best/1} \quad (56)$$

10. Compute $OF_k^{i+1} = F[u]_{k,D}^{i+1}$
11. Update the best values of (u_k^{best}) and (OF_k^{best})
12. End

Pseudocode of the Multi-Variant Differential Evolution Algorithm is shown in Table 4 [48]

Table.4 Pseudo-codes of the Multi-Variant Differential Evolution Algorithm (MVDE) method

Method: MVDE method

1. Generate an initial uniformly distributed random population consisting of n solutions containing d variables using:
   $x_{ij} = \text{rand}[0,1] \cdot \left(x_j^{max} - x_j^{min}\right) + x_j^{min} \quad \forall\ i \in \{1,2,\dots,NP\};\ j \in \{1,2,\dots,d\}$
2. Compute Xbest
3. Until the termination condition is not met
4. For t=2 to g
5. Slope=t/2/g;//mutation
6. For i < n
7. If rand > 3 ∗ Slope
8. $F_{ij} = F_{ij}.Ind_{ij}$;
9. End if
10. $CR = g/(2G)$ // $crossover$
11. if CR > Slope
12. $F_{ij} = CR.* F_{ij}$
13. Else
14. $N_p = n * (1 - CR)$ // selection
15. End if
16. If t < 0.2 ∗ g
17. $x_{ig} = x_{r1g}^{i} + F.(x_{r2g}^{i} - x_{r3g}^{i}) + F.(x_{r4g}^{i} - x_{r5g}^{i})$; //DE/rand/2
18. Else If t < 0.4 ∗ g
19. $x_{ig} = x_{r1g}^{i} + F.(x_{r2g}^{i} - x_{r3g}^{i})$; /DE/rand/1
20. else If t < 0.6 ∗ g
21. $x_{ig} = x_{ig} + F.\left(x_{best.g} - x_{ig}\right) + F(x_{r2g}^{i} - x_{r3g}^{i})$; //DE/target-to-best/1
22. Else If t < 0.8 ∗ g
23. $x_{ig} = x_{best,g} + F(x_{r1g}^{i} - x_{r2g}^{i}) + F(x_{r3g}^{i} - x_{r4g}^{i})$; //DE/ best/2
24. else
25. $x_{ig} = x_{best,g} + F(x_{r1g}^{i} - x_{r2g}^{i}$; //DE/ best/1
26. End if
27. End for
28. End while
29. Return the best solution

6. Simulation results based on MVDE method

Optimal allocation problem of mix of different types of distributed energy resources (DERs) units is solved based on Multi-variant differential evolution (MVDE) in different test cases for exploring. An analytical software tool has been created in MATLAB to perform load flow analysis and identify the best locations and sizes of Distributed Energy Resources (DERs). The study scenarios based on the annual growth load and numbers of objective functions are tabulated in Table 5. The network implemented in this work consists of 33 and 69 buses with

a base voltage of 12.66 kV, this system is optimized based on single objective functions, and multi-objective functions. Fig. 2 displays the subject's overall trend.

Table.5 Different cases studies investigated in this paper.

Scenario #	DERs	Case #	Y Value	System
1	PVs	Case 1	0	IEEE 33 bus
		Case 2	1	
		Case 3	2	
		Case 4	3	
		Case 5	4	
		Case 6	5	
2	WTs	Case 7	0	
		Case 8	1	
		Case 9	2	
		Case 10	3	
		Case 11	4	
		Case 12	5	
3	PVs &WTs &MTs &FCs	Case 13	0	
		Case 14	1	
		Case 15	2	
		Case 16	3	
		Case 17	4	
		Case 18	5	
4	WTs	Case 19	0	IEEE 69 bus
		Case 20	1	
		Case 21	2	
		Case 22	3	
		Case 23	4	
		Case 24	5	

- **IEEE 33 bus radial distribution system**

[49, 50] The IEEE 33 bus system, a typical small electrical energy network with 33 buses and 32 branches, is the system under discussion. It has a total load demand of 3.715 MW and 2.300 MVAR at 12.6 KV. Figure 3 illustrates a radial distribution network using IEEE 33-bus [51].

Over a five-year period, the impact of yearly increases in system load demand on bus voltages and power loss for every branch is examined. Figure 4 illustrates this effect without the integration of DERs units. It shows that when the system load demand increases annually, the voltage at each bus decreases and the branch losses rise.

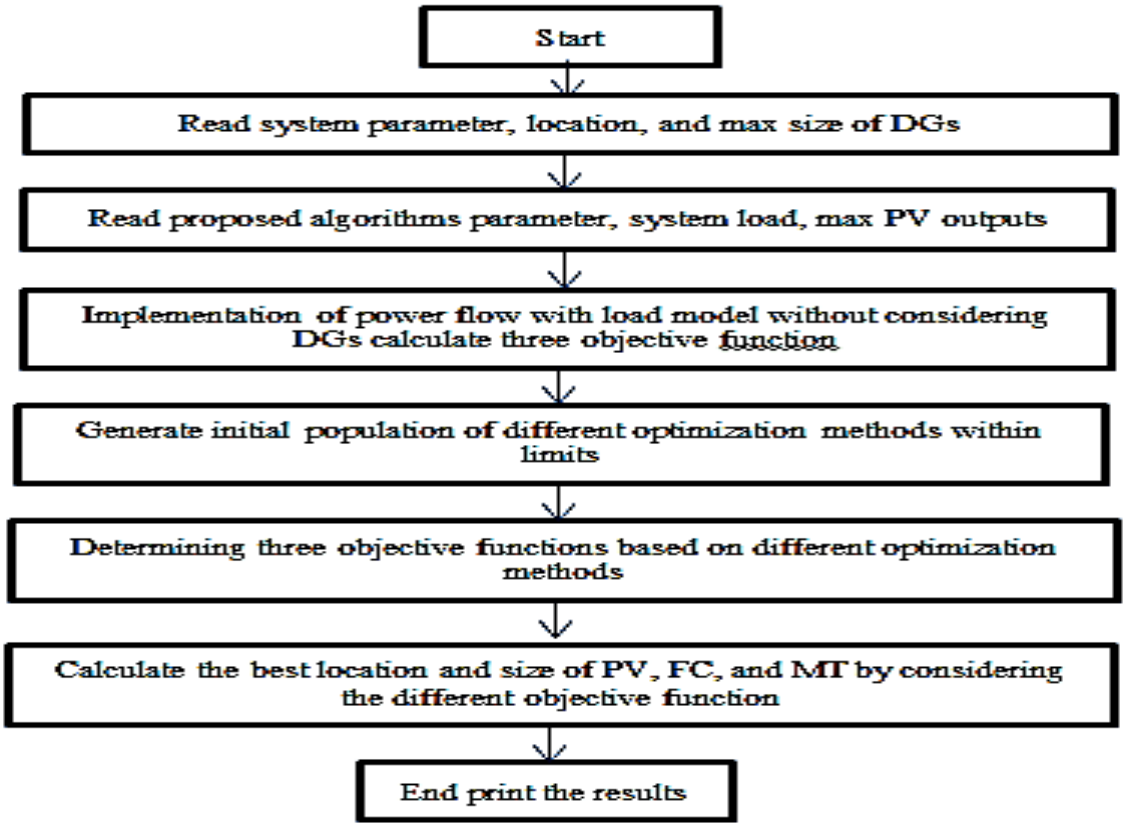

Fig 2. Overall solution procedure.

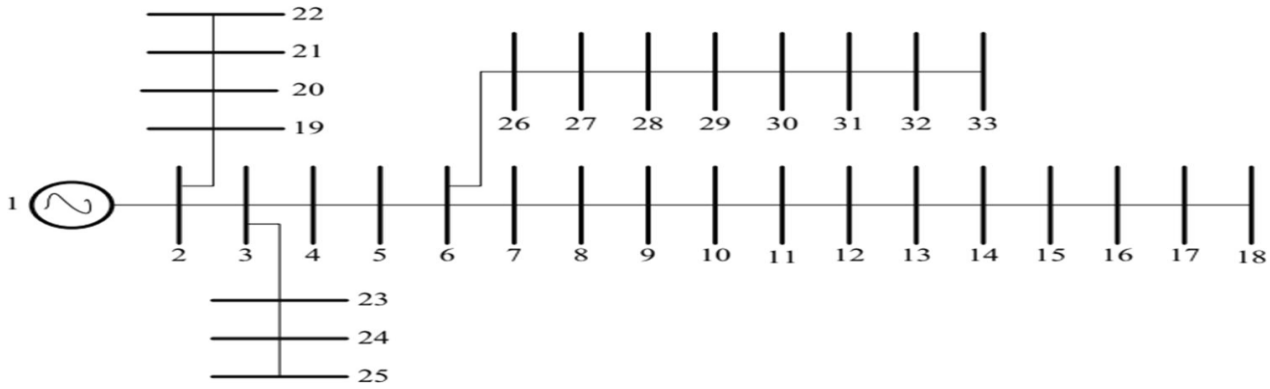

Fig 3. IEEE 33-bus radial distribution network

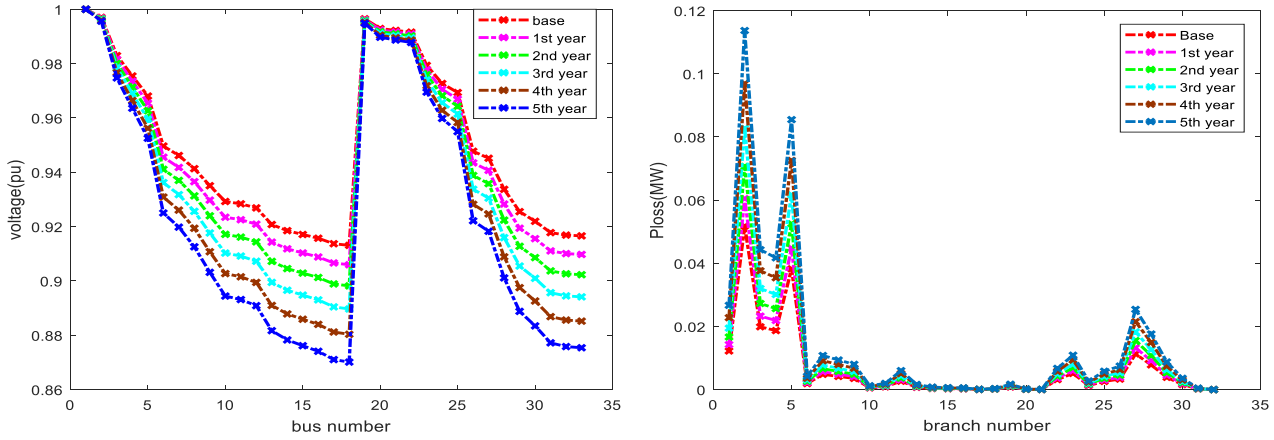

(a) Voltage profile (b) Power loss

Fig 4. System performance under annual load growth without integration DERs

6.1 Scenario 1: Allocating PV power generation system

a) Case 1 at y = 0

This instance uses MVDE methodologies to examine a system's performance for the base year. Table 6 shows the optimization results with and without PV units. It is evident that the minimum voltage raised to 0.96867 (33) p.u. and the power loss was reduced by 64.721%. The overall emissions are now 6129.4803 Ib/h instead of 8022.1 Ib/h. The 301st, 13th, and 24th buses are the best places to integrate three PV modules.

Table.6 Optimization results obtained at y=0

Case #		PV sizes MW, (location (bus no))	P_{loss} KW	Q_{loss} KVA	VD (PU)	V_{min} (location)	E_grid (Ib/h)
1	Without DERs	-	202.7	135.2	0.1171	0.9131(18)	8022.1
	With DERs	1.058(30) 0.78813(13) 1.0932(24)	71.51	49.42	0.01357	0.96867(33)	6129.4803

Figure 5 shows the improvement in the voltage profile and the decrease in power losses. With reference to Table 7, the suggested method may select the best placement and size for PV units while significantly reducing power losses and improving the voltage profile compared to the WOA, GA, SA, EAs, GA-PSO, ABC-CSO, ABC-BAT, ALO, and DOA algorithms that have been explored. The convergence curves, where MVDE achieves the least network power loss, are displayed in Fig. 6.

Table.7 comparison for IEEE 33 bus radial distribution system obtained for case 1

Algorithms	PVs sizes MW, (location (bus no))	P_{loss} KW	V_{min} (location)
MVDE	1.058(30); 0.78813(13); 1.0932(24)	71.51	0.96867(33)
WOA	1.2901(29); 0.57671(25); 0.72267(14)	74.5	0.96899(33)
GA	0.9464(11); 0.85462(25); 1.0196(30)	72.99	0.96594(18)
SA [25]	2.9356	70.189	0.95904(18)
EAs [30]	2.786	71.7	-
GA-PSO [36]	1496.7(30); 596.9(13); 234.6(10)	90.53	0.9689
ABC-CSO [36]	1265.7(30); 609.8(13); 198.4(10)	89.66	0.9701
ABC-BAT [36]	1360.8(30); 520.8(13); 148.5(10)	88.07	0.9742
ALO [36]	1323.5(30); 415.2(13); 130.2(10)	86.40	0.9767
DOA [37]	532(25); 866(33); 833(13)	78.62	0.96004(18)

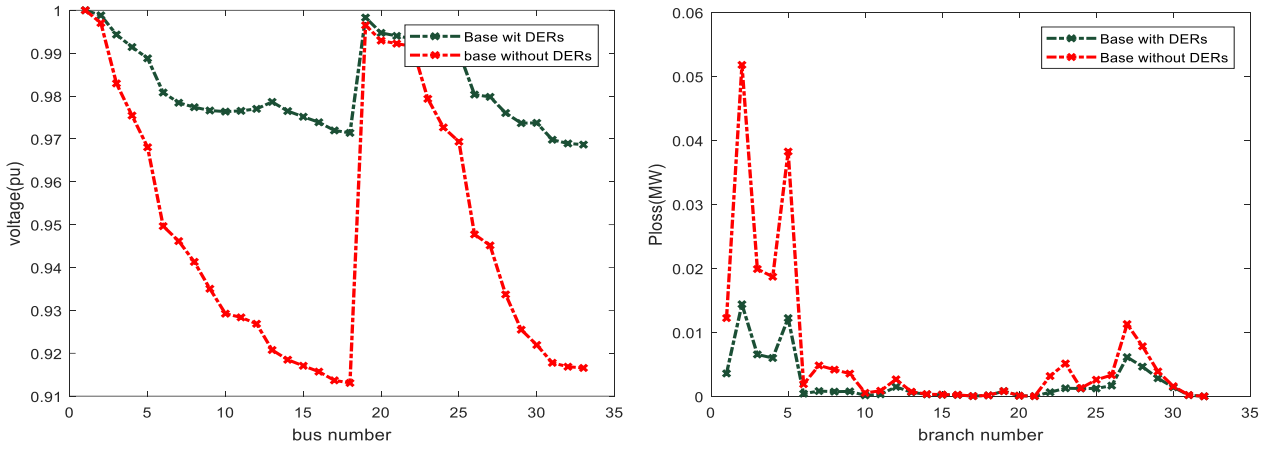

(a) Voltage profile (b) Power loss

Fig 5. System performance under annual load growth with integration DERs for base year

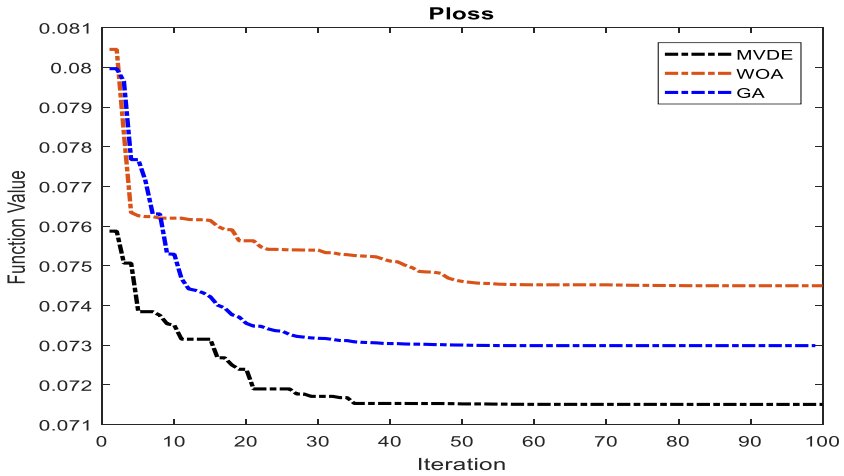

Fig 6. Performance comparisons of single-objective methods for case 1

b) Case 2 at y = 1

The annual growth of load demand at the first year is presented in this case; the annual load growth was handled via MVDE. From optimization results in Table 8, It is evident that the minimum voltage has been increased from 0.9059(18) p.u to 0.96628(33) p.u. The losses were decreased to 83.02 KW by installing total PV capacity of 3.2083 MW. The grid emission is reduced to 83.02 KW and 6598.3849 Ib/h.

In order to study the feasibility of the proposed solutions, voltage at each system bus and the power losses dissipated at each branch are presented in Fig. 7(a, b), respectively.

Table.8 The performance analysis of the proposed method results obtained at y=1

Case #		PV size MW, (location (bus no))	P_{loss} KW	Q_{loss} KVA	VD (PU)	V_{min} (location)	E_grid (Ib/h)
2	Without DERs	-	237.1	158.1		0.9059 (18)	8663
	With DERs	1.3081(30) 0.78998(13) 1.1102 (24)	83.02	57.39	0.01571	0.96625 (33)	6598.3849

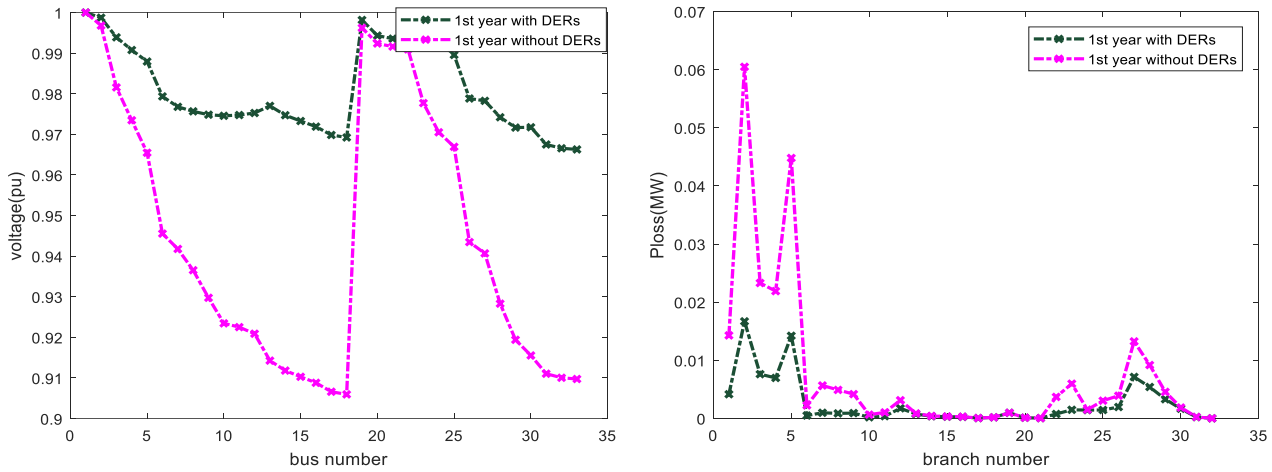

(a) Voltage profile (b) Power loss

Fig 7. System performance under annual load growth with integration DERs for first year

c) *Case 3 at y = 2*

The annual growth in system load demand through the second year (y=2) is displayed in this case. The optimization techniques at y=2, as tabulated in Table 9, it is also understood that the capacity of the best DG installations at the right site increases in direct proportion to the growth in load power demand. The inclusion of DERs is crucial for raising the minimum voltage to 0.99172 p.u. at bus 8 over the minimum permissible limits, since the bus voltages are lowered below the lowest allowable limits (Vmin = 0.8982 p.u. at bus 18). There was a 65.28% decrease in power loss. The amount of emissions dropped to 7112.4424 Ib/h.

After two years, it is found that the suggested algorithm significantly reduces power loss and enhances the voltage profile. Fig. 8(a, b) displays the voltage profile and power loss at each bus under the annual growth in system load demand.

Table.9 Optimization results obtained for second year

Case #		PV size MW, (location (bus no))	P_{loss} KW	Q_{loss} KVA	VD (PU)	V_{min} (location)	E_grid (Ib/h)
3	Without DERs	-	277.6	185.1		0.8982 (18)	9359.3
	With DERs	1.2451(30) 0.87376(13) 1.2763 (24)	96.38	66.63	0.01814	0.96373 (33)	7112.4424

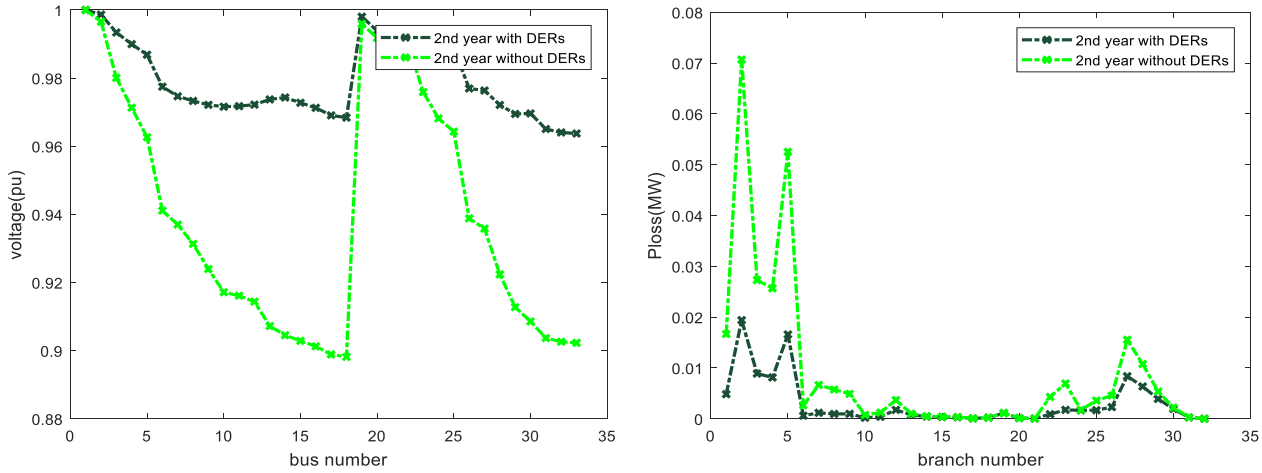

(a) Voltage profile (b) Power loss

Fig 8. System performance under annual load growth with integration DERs for second year

d) Case 4 at y = 3

A suggested approach for determining the optimal distribution of three PV units based on third years (y=3) is offered. Table 10 displays the optimization results from the optimization algorithm at y=3. It is clear that both the overall power loss and emissions are dropping to 122 KW and 7659.5978 Ib/h, respectively. Because of the yearly increase in network load requirement during the third year, the sizes of PV units are growing to 94.061, 1341, and 1374.5 KW. In order to study the feasibility of the proposed method for minimizing power loss and improving voltage profile, the voltage at each bus and power loss at each branch after integrating PVs units with good size and location are plotted in Fig. 9(a) and Fig. 9(b), obviously, the proposed method achieves a good performance for improving voltage profile and reducing power loss.

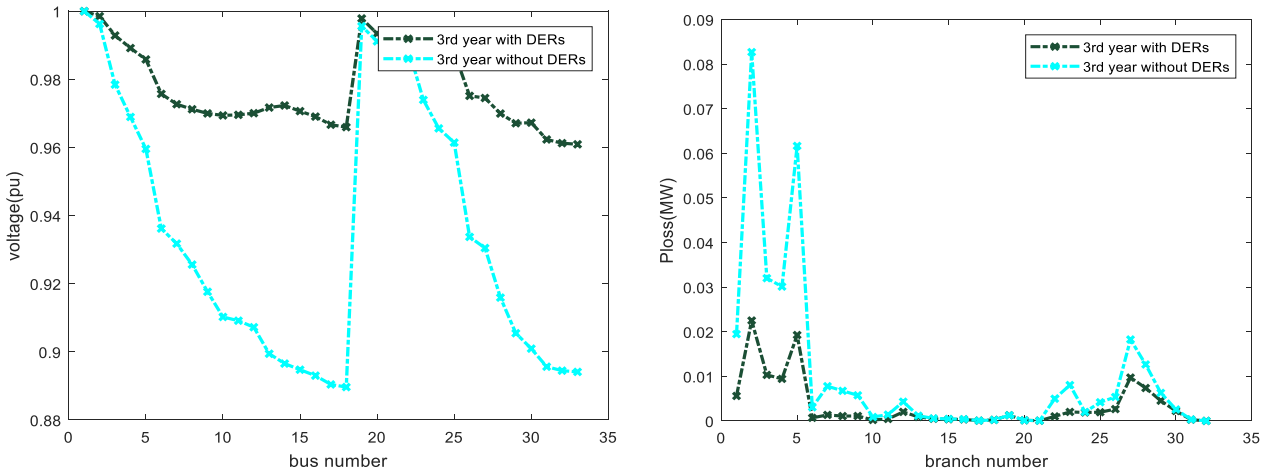

(a) Voltage profile (b) Power loss

Fig 9. System performance under annual load growth with integration DERs for third year

Table.10 Optimization results obtained at y=3

Case #		PV size MW, (location (bus no)	P_{loss} KW	Q_{loss} KVA	VD (PU)	V_{min} (location)	E_grid (Ib/h)
4	Without DERs	-	325.4	217.1		0.8897 (18)	10117
	With DERs	1.341(30) 0.94061(13) 1.3745(24)	112	77.44	0.02105	0.6092 (33)	7659.5978

e) Case 5 at y = 4

This case illustrates the annual growth of load demand at fourth year. The proposed multi-objective optimization methods are employed to reduce the total system power loss, total emission and voltage deviation, simultaneously, by allocating three PV units. After combining three units of PVs with a total size of 3.9562 MW, it is evident from the optimization findings in Table 11 that the minimum voltage increased from 0.8803 p.u. to 0.95794 p.u. The best location for PV is close to buses (13, 24, 30). The power losses have been reduced by 34 %, and voltage deviation is reduced to 0.02439p.u. the minimum value of three objective functions ($F_1 = 130.22$ KW , $F_2 = 0.02439$p. u and $F_3 = 8248.8276$ Ib/h),

The feasibility of the proposed solutions is illustrated in Fig. 10(a), and Fig. 10(b), where system power loss minimization and voltage deviation reduction are shown, respectively.

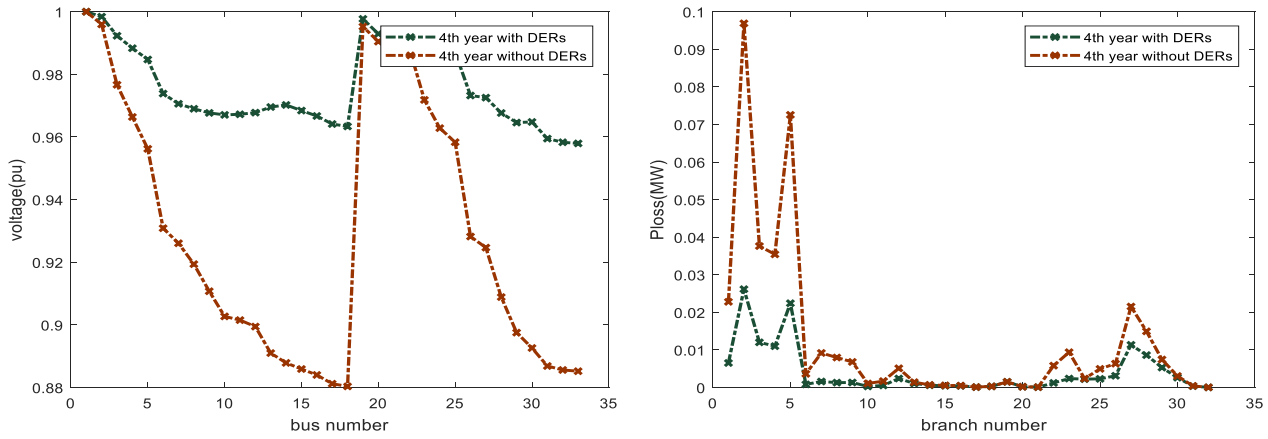

(a) Voltage profile (b) Power loss

Fig 10. System performance under annual load growth with integration DERs for forth year

Table.11 Optimal allocation of PVs units for case 5

Case #		PV size MW, (location (bus no))	P_{loss} KW	Q_{loss} KVA	VD (PU)	V_{min} (location)	E_grid (Ib/h)
5	Without DERs	-	382.1	255		0.8803 (18)	10941
	With DERs	1.446(30) 1.029(13) 1.4811 (24)	130.22	90.04	0.02439	0.95794 (33)	2024.0761

f) Case 6 at y = 5

In this case, the effectiveness of the MVDE technique has been evaluated and demonstrated considering load growth at fifth year (5th year), the voltage profile and the loss of the network

are shown in Fig 11(a) and Fig. 11(b), respectively. The behavior of the system at y=5 is depicted in Table 12, the power loss is reduced from 449.5 KW to 151.47 KW, and the minimum voltage increased from 0.8701 p.u. at 18th bus to 0.95472 p.u at 33th bus. The total emissions are reduced from 11841 Ib/h to 8884.8029 Ib/h.

Table.12 Optimization results obtained for fifth year

Case #		PV size MW, (location (bus no))		P_{loss} KW	Q_{loss} KVA	VD (PU)	V_{min} (location)	E_grid (Ib/h)
6	Without DERs	-		449.5	300		0.8701 (18)	11841
	With DERs	1.5592(30) 1.5967(24)	1.0908(13)	151.47	104.75	0.02827	0.95472(33)	8884.8029

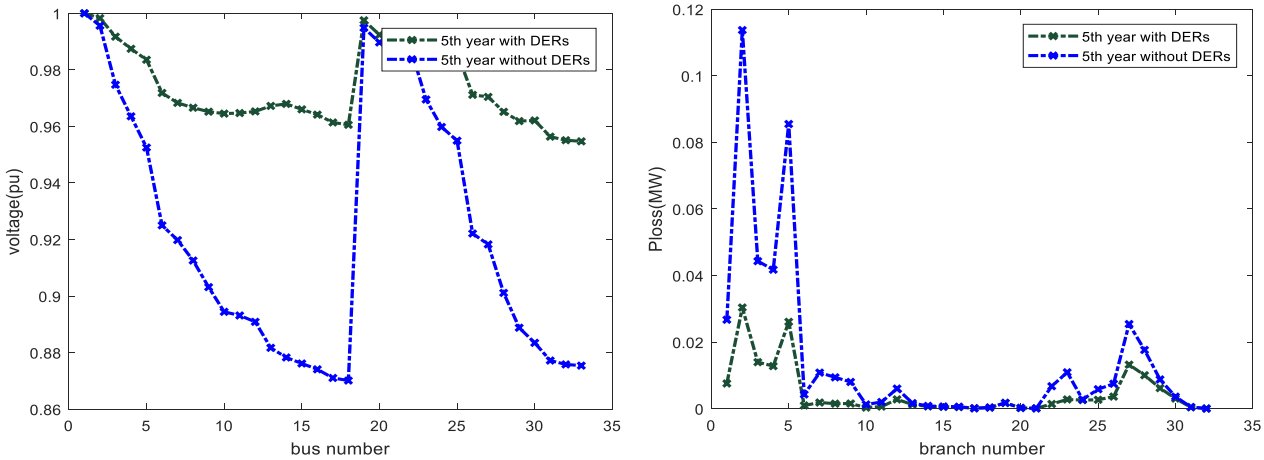

(a) Voltage profile (b) Power loss

Fig 11. System performance under annual load growth with integration DERs for fifth year

6.2 Scenario 2: Allocating WT power generation system

In this scenario, MVDE algorithm determines the best placement and size of the three WT units taking into account the ability to reduce power losses.

a) Case 7 at y = 0

This case uses MVDE methodologies to examine a system's performance for the base year. Table 13 shows the optimization results with and without the use of WT units. It is evident that the minimum voltage increases from 0.9131 (18) p.u. to 0.99289 (8) p.u. and the power loss decreases from 202.7 KW to 14.42 KW. The overall emissions are lowered to 1571.1554 Ib/h from 8022.1 Ib/h. Because WT units produce both active and reactive power, the minimum voltage and overall size obtained in this example are higher than the results obtained in scenario 1. The 301st, 13th, and 24th buses are the best places to add three WTs units, the improvement in voltage profile and the reduction in power losses are illustrated in Fig.12. Referring to Table 14, the proposed approach (MVDE) is able to choose the optimal location and size of WTs units operating at the optimum power factor with a significant saving of power losses, and improvement of voltage profile enhancement than studied GA-PSO, ABC-CSO, ABC-BAT and ALO algorithms.

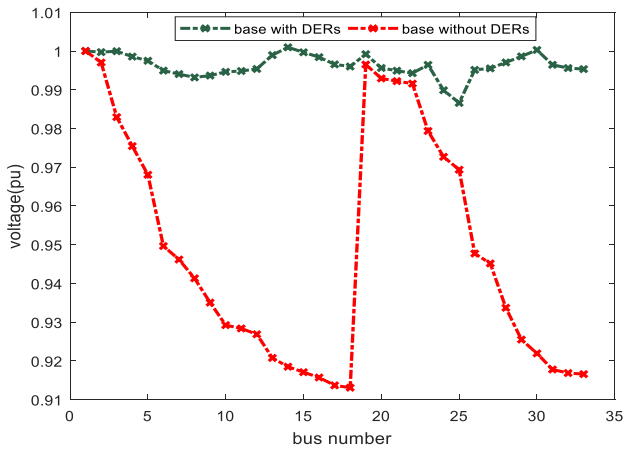

(a) Voltage profile

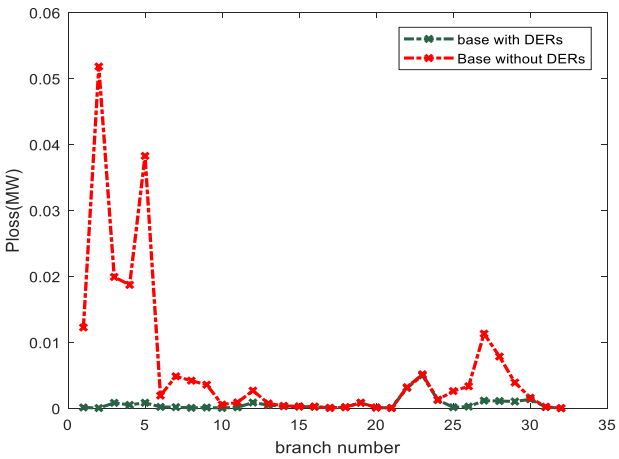

(b) Power loss

Fig 12. System performance under annual load growth with integration DERs for base year

Table.13 Optimization results obtained at y=0

Case #		WT size MW, (location (bus no))/ PF	P_{loss} KW	Q_{loss} KVA	VD (PU)	V_{min} (location)	E_grid (Ib/h)
7	Without DERs	-	202.7	135.2	0.1171	0.9131(18)	8022.1
	With DERs	1.2094(30)/0.85 0.7502(13)/0.86698 1.0025(24)/0.8587	14.4	11.75	0.00057	0.99289(8)	1571.1554

Table.14 Performance comparison with multiple WTs units

Algorithms	MVDE	GA-PSO [36]	ABC-CSO [36]	ABC-BAT [36]	ALO[36]
WT size MW, (location (bus no))/ PF	1.2094(30)/0.85 0.7502(13)/0.86698 1.0025(24)/0.8587	1425.7(30)/0.866 639.6(13)/0.866 168.4(10)/0.866	1394.1(30)/0.866 553.1(13)/0.866 296.8(10)/0.866	1336.2(30)/0.866 465.9(13)/0.866 201.2(10)/0.866	1225.2(30)/0.866 610.4(13)/0.866 269.1(10)/0.866
P_{loss} KW	14.4	37.08	36.61	34.43	31.65
V_{min} (location)	0.99289(8)	0.9712	0.9763	0.9798	0.9802

b) Case 8 at y = 1

In this case an increase in the load level raises all objective values and boosts the WT units' overall capacity. In comparison to case 7, the WT units' size grew from 2.9621 MW to 3.20825 MW. The total losses reduced to 16.64 MW refer to optimization results in Table 15. The minimum voltage reduced from 0.9131p.u at the base year to 0.9059 p.u without integrating WTs units, after integrating WTs units this value increased to 0.99242 p.u, grid emission is reduced to 1642.1158 Ib/h. The feasibility of the proposed solutions is illustrated in Fig. 13 (a) and Fig. 13 (b), where the improvements in the voltage profile and system power loss are shown, respectively.

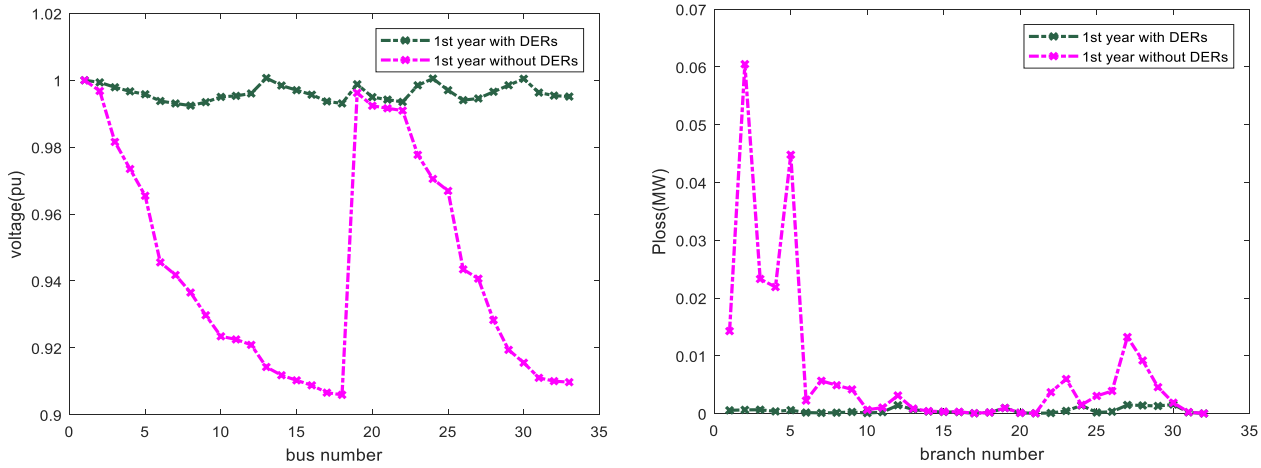

(a) Voltage profile (b) Power loss

Fig 13. System performance under annual load growth with integration DERs for first year

Table.15 Optimization results obtained at y=1

Case #		WT size MW, (location (bus no))/ PF	P_{loss} KW	Q_{loss} KVA	VD (PU)	V_{min} (location)	E_grid (Ib/h)
8	Without DERs	-	237.1	158.1		0.9059 (18)	8663
	With DERs	1.3081(30)/0.85 0.78998(13)/0.85715 1.1102 (24)/0.87105	16.64	13.6	0.010246	0.99242 (25)	1642.1158

c) Case 9 at y = 2

This case displays the annual growth in system load demand through the second year (y=2). The performance of network at y=2 is found in Table 16, from the optimization result, the bus voltages are reduced below the minimum allowable limits (Vmin = 0.8982 p.u at bus 18), Inclusion of DERs is important for increasing minimum voltage to 0.99172 p.u at bus 8 upper the minimum allowable limits. The power loss and emissions reduced by 93.08 % and 80.759 %, respectively. Figure 14(a) and Figure 14(b) show the voltage profile and power loss under the annual growth in system load demand during the second year, respectively. It is found that the MVDE algorithm significantly improves the voltage profile and reduces power loss.

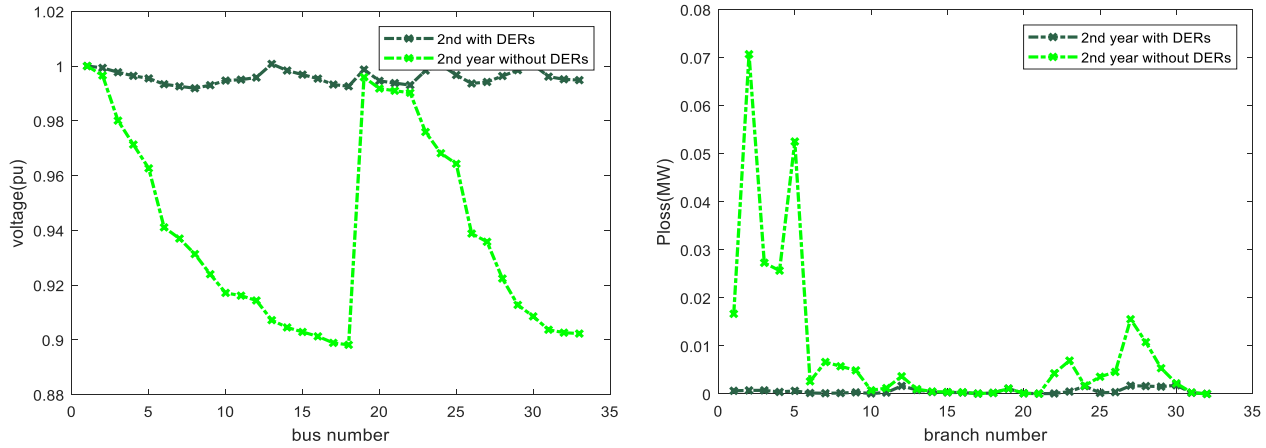

(a) Voltage profile (b) Power loss

Fig 14. System performance under annual load growth with integration DERs for second year

Table.16 Simulation Results after WTs units Placement for y=2

Case #		WT size MW, (location (bus no))/ PF		P_{loss} KW	Q_{loss} KVA	VD (PU)	V_{min} (location)	E_grid (Ib/h)
9	Without DERs	-		277.6	185.1		0.8982 (18)	9359.3
	With DERs	1.40363(30)/0.85002 0.85249(13)/0.86194 (24)/0.86119	1.1742	19.2	15.75	0.20367	0.99172 (8)	1800.7619

d) Case 10 at y = 3

MVDE method is presented to find the best allocation of three units of WTs units based on third years (y=3). The optimization results obtained from the optimization algorithm at third year are tabulated in Table 17, it's evident that the total power loss and emission are decreasing and the WTs unit sizes are increasing due to annual growth in network load demand during the third year. Figure 15(a) and Figure 15(b) illustrate the bus voltage and the power loss following the use of WT units of appropriate size and location in order to assess the viability of the suggested approach. It is clear that the MVDE method performs well in terms of improving the voltage profile and lowering power loss.

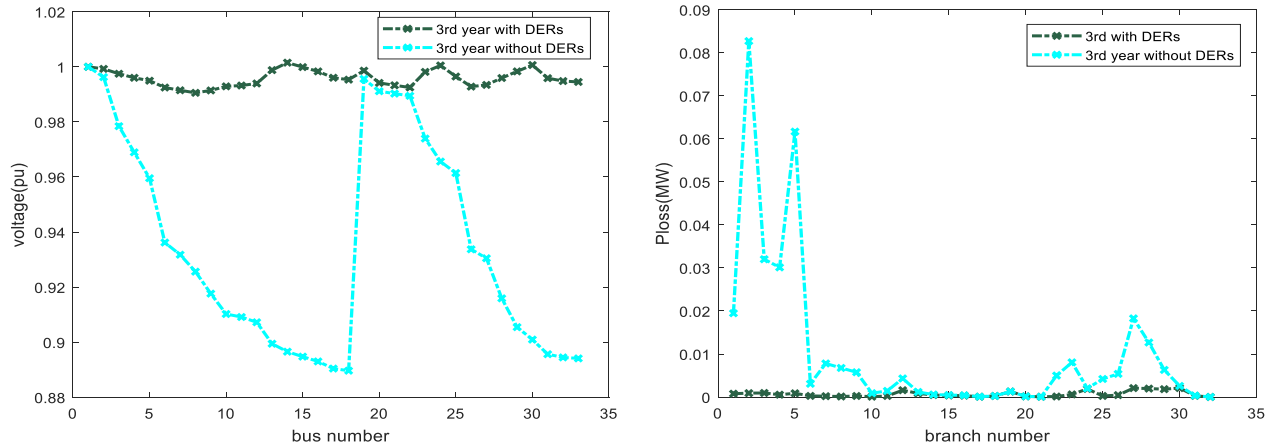

(a) Voltage profile (b) Power loss

Fig 15. System performance under annual load growth with integration DERs for third year

Table.17 The best allocation of three units of WTs units based on third years

Case #		WT size MW, (location (bus no))/ PF	P_{loss} KW	Q_{loss} KVA	VD (PU)	V_{min} (location)	E_grid (Ib/h)
10	Without DERs	-	325.4	217.1		0.8897 (18)	10117
	With DERs	1.518(30)/0.85 0.91337(13)/0.85674 1.28911(24)/0.87323	22.22	18.2	0.00085	0.9913 (8)	1894.0644

e) Case 11 at y = 4

In this case, the proposed method is used to determine the optimal location and size of three WT units considering minimization of the network power losses, emission, and voltage deviation. It is seen that the proposed algorithm achieves remarkable in minimizing the total system power losses with acceptable minimum voltage, as shown in Table 18. The minimum voltage increased from 0.8803 p.u to 0.99073 p.u, after integrating three units of WTs, power loss and grid emission are reduced to 25.75 KW and 2024.0761 Ib/h, respectively. Figure 16(a) shows the voltage profile at each bus, and Figure 16(b) shows the power loss at each bus.

Table.18 Optimization results for fourth year

Case #		WT size MW, (location (bus no))/ PF	P_{loss} KW	Q_{loss} KVA	VD (PU)	V_{min} (location)	E_grid (Ib/h)
11	Without DERs	-	382.1	255		0.8803 (18)	10941
	With DERs	1.6349(30)/0.85 0.98041(13)/0.85495 (24)/0.8736 1.3832	25.75	21.07	0.00096	0.99073 (8)	2024.0761

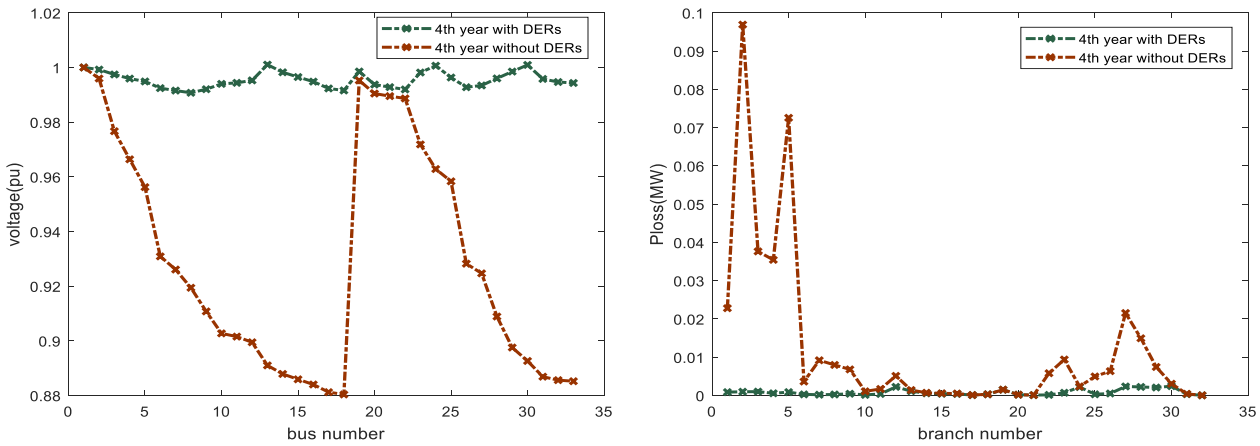

(a) Voltage profile (b) Power loss

Fig 16. System performance under annual load growth with integration DERs for forth year

f) Case 12 at y = 5

In this case, the optimal optimization results are obtained for the fifth year (5th year), The feasibility of the proposed solutions is illustrated in Fig. 16 (a) and Fig. 16 (b), where the improvements in the voltage profile and system power loss are shown, respectively. The final

simulation results are listed in Table 18, the power loss is reduced from 449.5 KW to 29.79 KW, and the minimum voltage deviation is increased to 0.99017 p.u. The total emissions are reduced from 11841 Ib/h to 2145.0529 Ib/h.

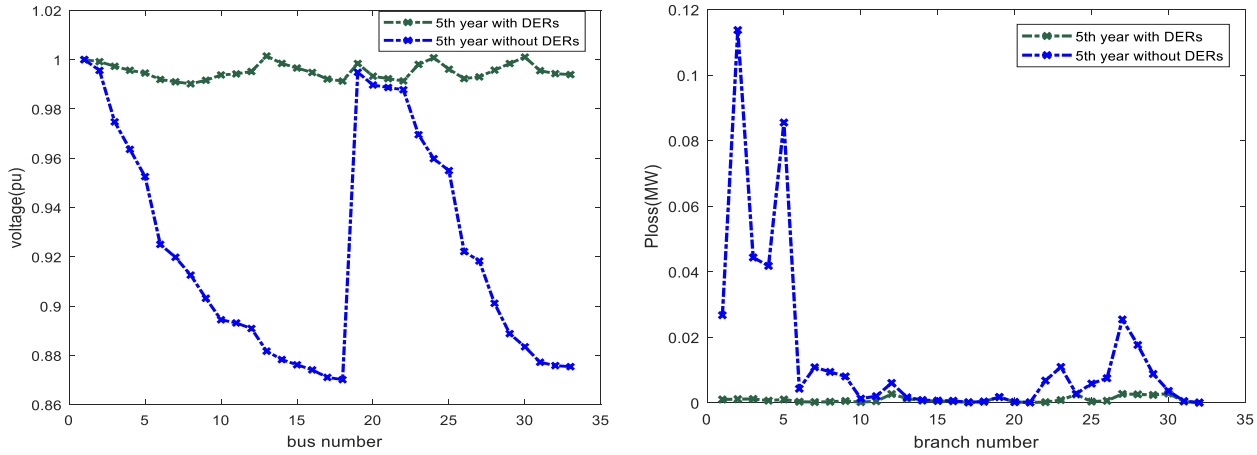

(a) Voltage profile (b) Power loss

Fig 17. System performance under annual load growth with integration DERs for fifth year

Table.19 Optimization results obtained at y=5

Case #		WT size MW, (location (bus no))/ PF		P_{loss} KW	Q_{loss} KVA	VD (PU)	V_{min} (location)	E_grid (Ib/h)
12	Without DERs	-		449.5	300		0.8701 (18)	11841
	With DERs	1.756(30)/0.85 1.063(13)/0.85693 (24)/0.87718	1.4966	29.79	24.36	0.00107	0.99017 (8)	2145.0529

6.3 Scenario 3: Allocating Hybrid Renewable Energy Resources

In this scenario, the planning of hybrid power system model is presented with the load growth. A hybrid renewable energy resources (RERs) like photovoltaic system (PV), wind turbine system (WT) and nonrenewable energy resources (N-RERs) such as micro-turbine (MT), and fuel cell (FC) are integrated in a system to supply energy demand based on proposed methods to maximize technical, economic, and environmental benefits of DERs. The results optimized by the suggested method are listed in Table 20, It is clearly seen that the total capacity of each unit of DERs increases due to increase in the load demand through five years.

The three objective functions together in 3-dimensional space, power losses dissipated at each branch and voltage at each system bus due to annual growth in network load demand through five years are investigated in Fig.18, Fig.19 (a), and Fig.19 (b), respectively. From Fig.18, Fig.19 (a), it is observed that the different objectives and loss at each branch increase with annual load growth. Referring to Fig.19 (b), it is obvious that the network voltages decrease with the load growth.

Table.20 The performance analysis of the proposed method for scenario 3

Y	F_1 KW	Q_{loss} KVA	VD (PU)	F_2 $/h	F_3 Ib/h	FC size (bus no)	MT size (bus no)	PV size (bus no)	WT size (bus no)
Y=0	75.0668	51.1182	0.6555	180.41553	5115.79947	0.20148(12) 0.25(27) 0.21055(33) 0.25(3)	0.21283(17) 0.4(32) 0.4(20) 0.3706(26)	0.16293(16) 0.14248(5)	0.058379(29) 0.061469(13)
Y=1	92.7146	62.1109	0.7501	191.4882	6095.21414	0.23544(16) 0.2013(33) 0.23923(26) 0.19552(31)	0.16456(27) 0.35062(7) 0.28445(10) 0.20382(13)	0.13624(17) 0.16842(21)	0.058768(8) 0.063903(28)
Y=2	113.0259	75.7030	0.9998	205.51437	6690.02649	0.23541(10) 0.067581(8) 0.25(15) 0.18685(20)	0.4 (31) 0.15324(15) 0.32815(30) 0.34226(26)	0.16682(3) 0.17615(27)	0.059204(17) 0.049254(12)
Y=3	127.3115	85.4744	1.0639	222.07465	7245.42798	0.25(6) 0.25(26) 0.25(30) 0.09412(4)	0.4(25) 0.0063001(3) 0.4(17) 0.4(9)	0.14643(15) 0.16128(33)	0.067911(32) 0.05896(19)
Y=4	167.6739	111.5440	1.2903	234.56600	8359.08685	0.25(8) 0.25(29) 0.22004(12) 0.25(32)	0(30) 0.18611(6) 0.28386(31) 0.26313(14)	0.17549(2) 0.17135(33)	0.06198(10) 0.065(11)
Y=5	194.2980	128.0921	1.3345	257.09819	8971.38182	0.25(12) 0.18392(16) 0.18355(7) 0.20066(10)	0.30756(31) 0.39763(32) 0.19744(33) 0.23201(19)	0.15561(15) 0.13337(11)	0.061067(14) 0.06187(21)

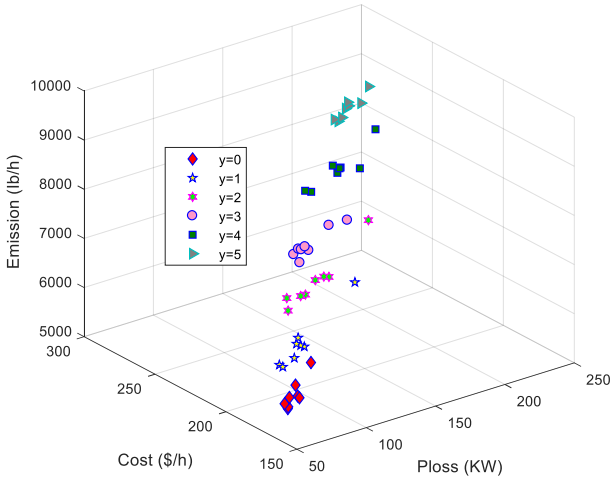

(a)

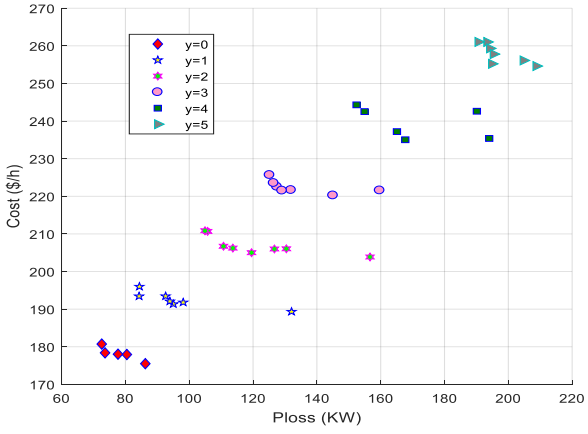

(b)

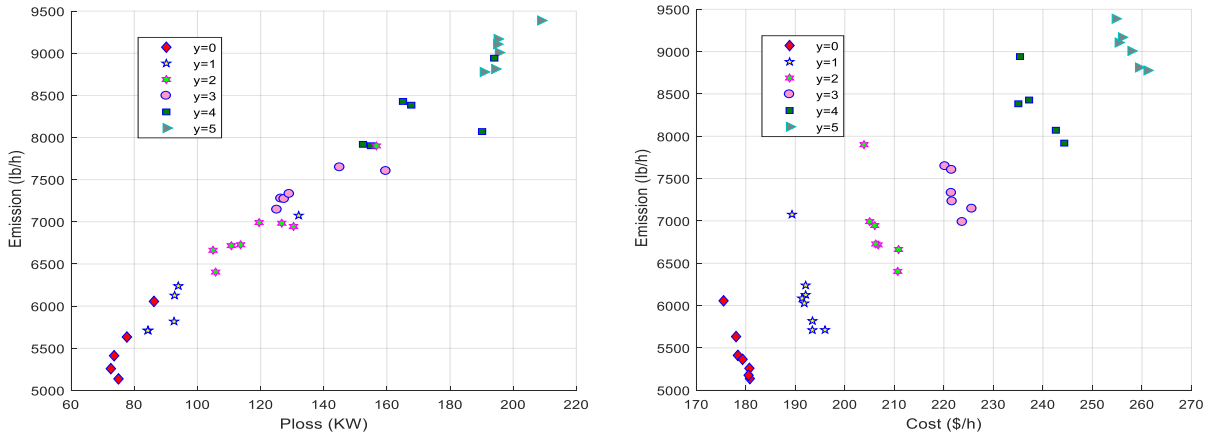

(c) (d)

Fig 18. Pareto frontiers and 2-D projections for scenario 3

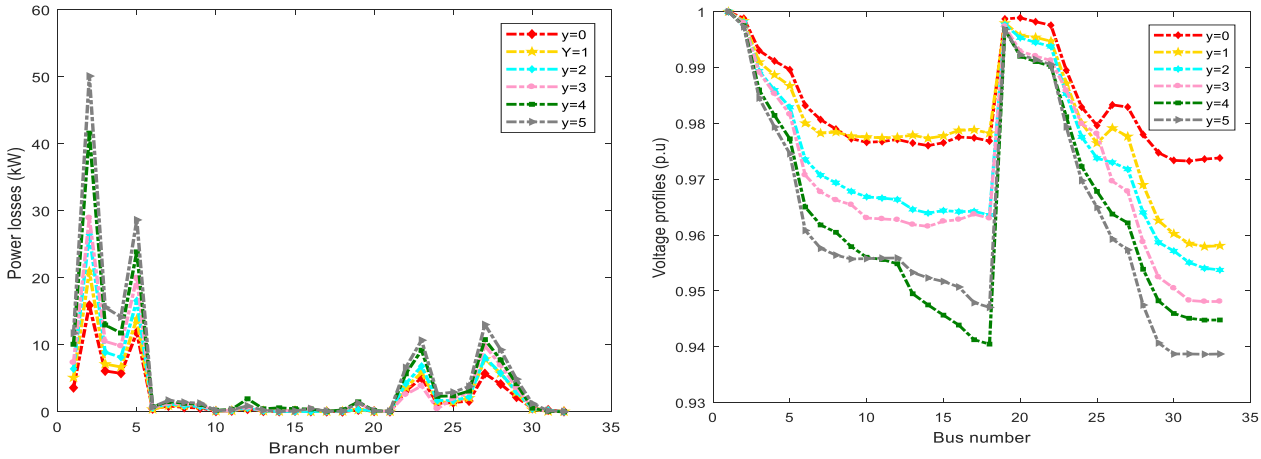

(a) Power loss (b) Voltage profile

Fig 19. Performance of the system over load growth

a) Case 13 at y = 0

From Table 19 at base year the power losses are reduced from 202 KW to 75.0668 KW, the minimum voltage deviation is increased to 0.6555 p.u. The total emissions are reduced from 8022.1 Ib/h to 5115.79947 Ib/h. The optimal locations for inclusion PV renewable energy resources are the 16th and 5th bus, for inclusion PV renewable energy resources are the 29th and 13th bus.

Fig. 20 (a, and b) indicates the three objectives and the sizes of each energy resource at base case (y=0). The minimum loss is 72.57 KW, the cost and emissions related to this loss are 180.7 4 $/h, and 5258 Ib/h, respectively. To reduce power loss the cost and emissions in this case, the sizes of PV and WT units must be equal to 171.3, 143, 59.31, and 57.05, respectively.

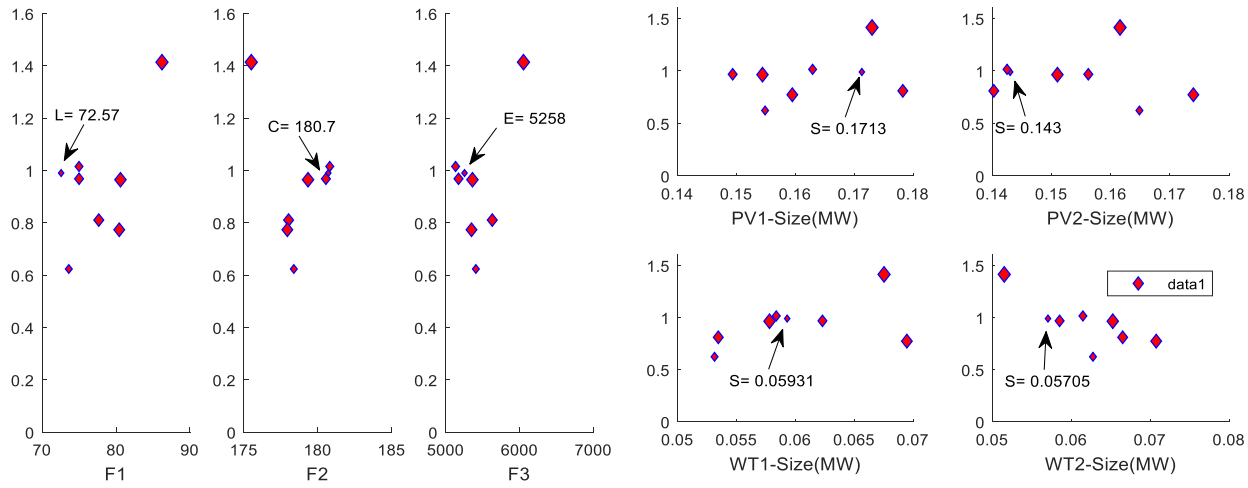

(a) (b)

Fig 20. The three objectives and the sizes of each energy resource at Y=0

b) Case 14 at y = 1

From Table 19 the power losses are increased from 75.0668 KW at base year to 92.7146 KW at first year, the total cost is increased from 180.41553 $/h at base year to 191.4882 $/h at first year p.u. The total emissions are increased from 5115.79947 Ib/h at base year to 6095.21414 Ib/h at first year. The optimal sizes for inclusion PV renewable energy resources are 136.24 and 168.42 KW, for inclusion WT renewable energy resources are 58.768 and 63.903 KW. Fig. 21 (a, and b) indicates the three objectives and the sizes of each energy resource at first case (y=1). It is observed that, after one year the values of all objectives and the sizes of energy resource increased with the increasing in the load. The minimum loss and the cost and emissions related to this loss are 84.28 KW, 193.4 $/h, and 5710 Ib/h, respectively. The sizes of PV and WT units are 146.8, 173.2, 59.2, and 63.93 KW, respectively.

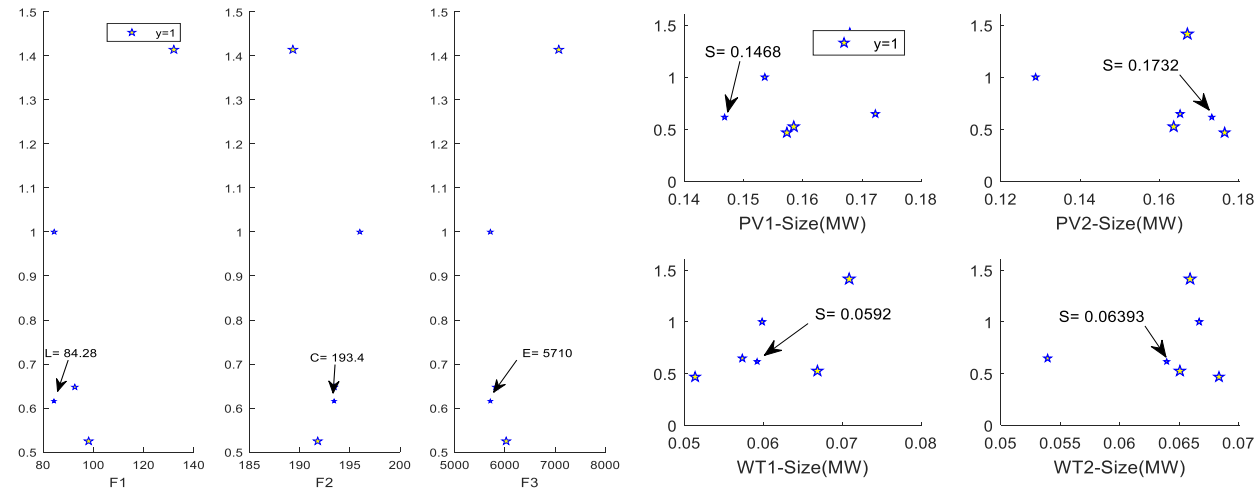

(a) **(b)**

Fig 21. The three objectives and the sizes of each energy resource at Y=1

c) Case 15 at y = 2

After two years, the proposed algorithm achieves best performances for minimizing power loss, cost and emissions in addition to improving the voltage profile, as given in Table 19.The

power losses, the total cost, and the total emissions are reduced to 113.0259 KW, 205.51437 $/h and 6690.02649 Ib/h. The optimal sizes for inclusion PV renewable energy resources are increased from 136.24 and 168.42 KW at first years to 166.82 and 176.15 KW at second years, for inclusion WT renewable energy resources are changed from 58.768 and 63.903 KW at first years to 59.204 and 49.25 KW at second years.

The three objectives and the sizes of each energy resource at second year (y=2) are illustrated in Fig. 22 (a, and b). It is observed that the minimum loss and the cost and emissions related to this loss are increased to 104.9 KW, 210.8 $/h, and 6663 Ib/h, respectively. The sizes of PV and WT units are 140.6, 155.2, 60.32, and 60.13 KW, respectively. large sizes of PV 2and the small sizes of PV 1 leads to minimize power losses and WT sizes are in the range [0.056 - 0.07] MW.

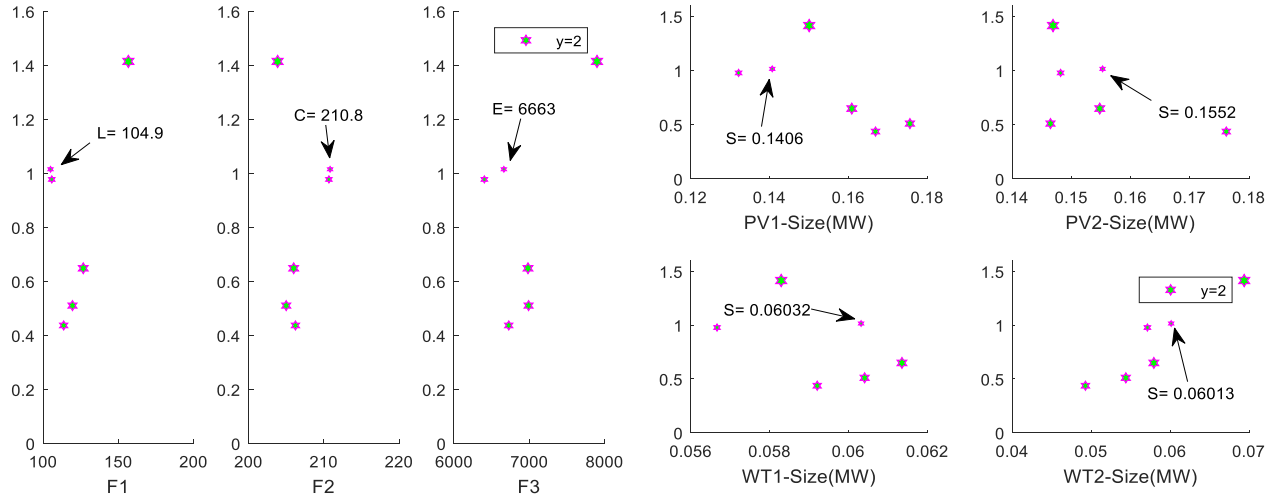

(a) (b)

Fig 22. The three objectives and the sizes of each energy resource at Y=2

d) Case 16 at y = 3

Optimally incorporating the DERs using the proposed method can maximize technical, economic and environmental benefits by reducing the power losses to 127.3115 KW, annual cost to 222.07465 $/h , and greenhouse gas to 7245.42798 Ib/h refer to Table 19.

The three objectives at third year (y=3) are shown in Fig. 23 (a). It is observed that the minimum loss and the cost and emissions related to this loss are 125.2 KW, 225.7 $/h, and 7145 Ib/h, respectively. The PV and WT sizes shown in Fig. 23 (b) are 176.8, 156.7, 51.98, and 63.9 KW, respectively. It is clear that the power loss will be reduced when the sizes of PV 1 and WT 2 are large, and the sizes of PV 2 and WT 1 are small.

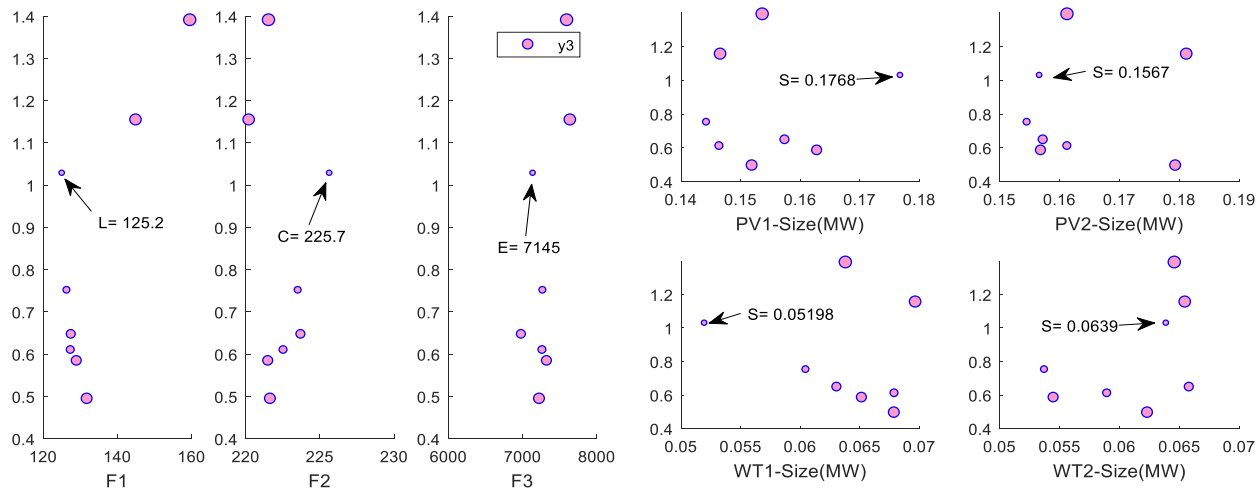

(a) (b)

Fig 23. The three objectives and the sizes of each energy resource at Y=3

e) Case 17 at y = 4

From Table 19 the power losses, the total cost, and the total emissions at 4th year equal to 167.6739 KW, 234.56600 $/h and 8359.08685 Ib/h, respectively. The optimal sizes and locations for inclusion renewable energy resources are 175.49, 171.35, 61.98, and 65 KW at 2nd, 33th, 10th, and 11th buses, respectively.

Fig. 24 (a, and b) shows the three objectives and the renewable energy resource sizes at fourth year (y=4). It is observed that the minimum loss and the cost and emissions related to this loss are increased to 152.4 KW, 244.3 $/h, and 7919 Ib/h, respectively. The sizes of PV and WT units are changed from 171.3, 143, 59.31, and 57.05 KW at base case (y=0) to 144.7, 144, 52.72, and 57.33 KW at fourth year (y=4), respectively.

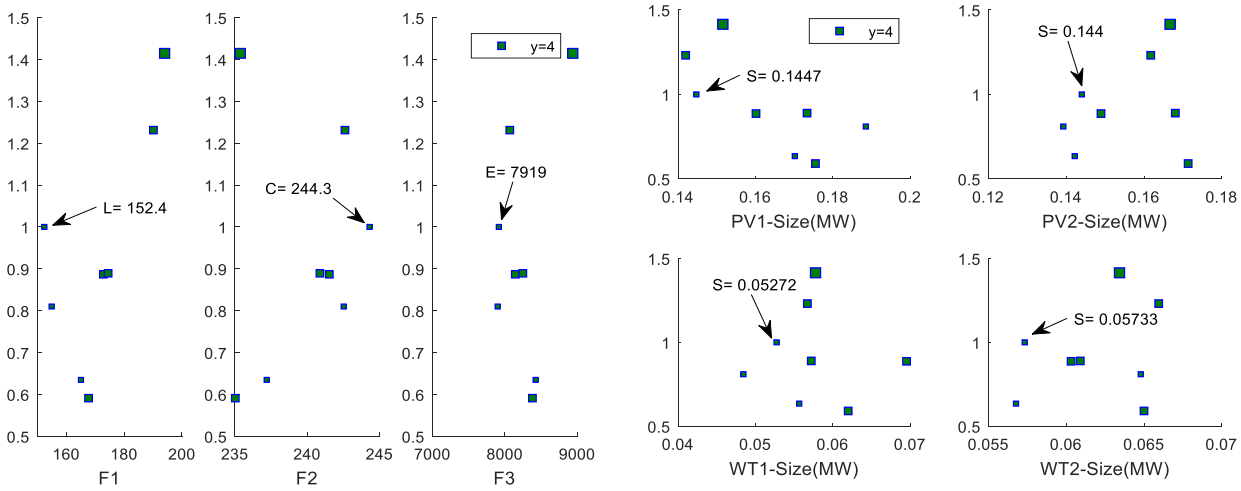

(a) **(b)**

Fig 24. The three objectives and the sizes of each energy resource at Y=4

f) Case 18 at y = 5

The optimal sizes and location of DERs obtained by the proposed optimization algorithm are tabulated in Table 19. It is observed that the proposed method is capable of selecting the optimal location and size of DERs with a significant saving of power losses and cost, and

reducing emission of the system. The power losses, annual cost, and greenhouse gas are 194.2980 KW, 257.09819 $/h, and 8971.38182 Ib/h.

The three objectives at fifth year (y=5) are shown in Fig. 25 (a). It is observed that the minimum loss and the cost and emissions related to this loss are 190.6 KW, 261 $/h, and 8778 Ib/h, respectively. The PV and WT sizes shown in Fig. 25 (b) are 156.6, 130.1, 61.08, and 62.53 KW, respectively, leads to improve the system performance.

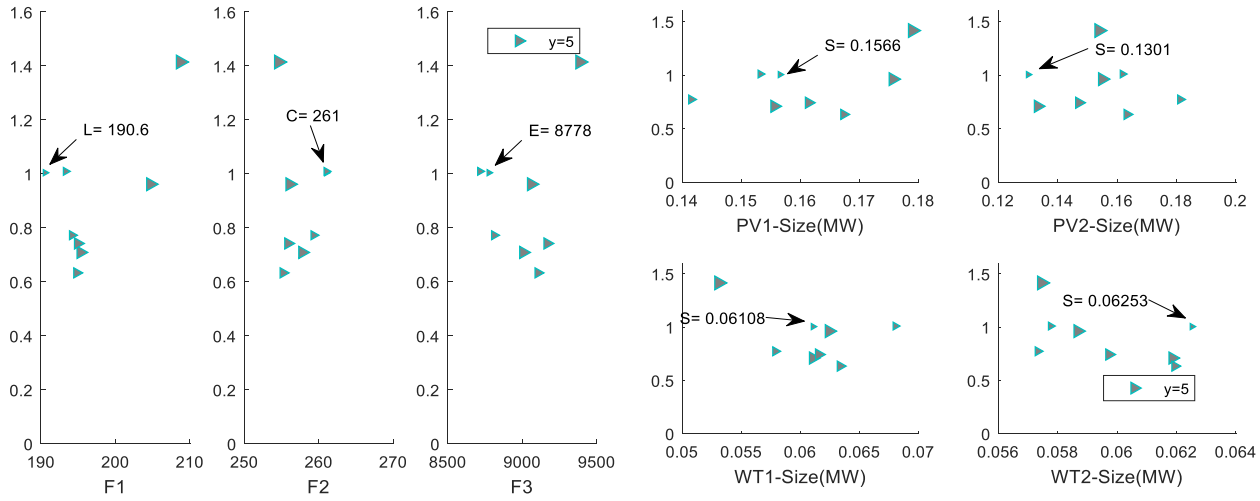

Fig 25. The three objectives and the sizes of each energy resource at Y=5

- **IEEE 69 bus radial distribution system**

The second study system is IEEE 69 bus-system, which is a standard and small electrical power network consists of 69 buses and 68 branches. The total real and reactive power loss of this case is 225 kW and 102.2 kVA respectively. The bus data and line data of this system are taken from [52]. IEEE 69-bus radial distribution network is shown in Fig. 26.

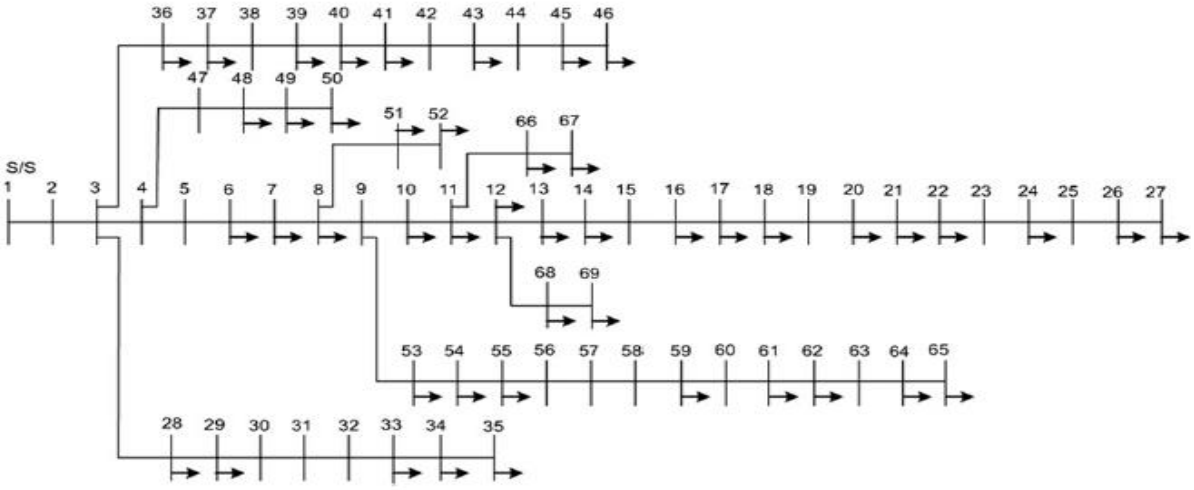

Fig 26. IEEE 69-bus radial distribution network

6.4 Scenario 4: Allocating WT power generation units

The effect of annual growth in system load demand on bus voltages and power loss for each branch over five years are investigated. This effect without the integration of WT units are

demonstrated in Figs. 27, it is observed that the voltage at each bus decreases and the branches losses increase with the annual growth in system load demand.

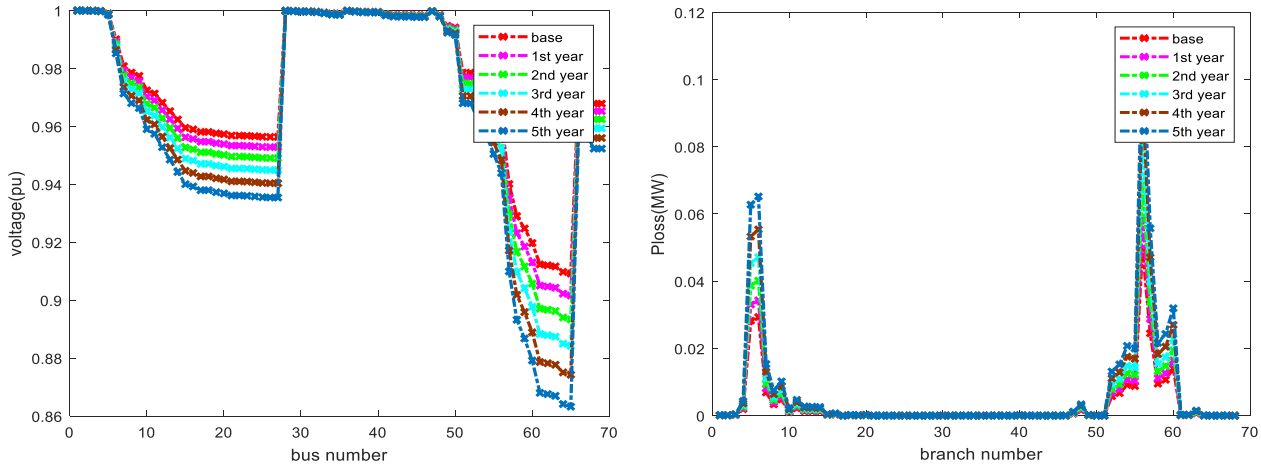

(a) Voltage profile (b) Power loss

Fig 27. System performance under annual load growth without integration DERs

a) Case 19 (y = 0)

This case analyzes the performance of a system for the base year based on ALO methods. The optimization results with and without WT units are given in Table 21, it's clear that the power loss is reduced by from 225 KW to 4.98 KW, the minimum voltage is increased from 0.9092(65) p.u to 0.99426(50) p.u. The optimal locations for inclusion three WTs units are the 61th, 11th, and 18th bus, the improvement in voltage profile and the reduction in power losses are illustrated in Fig.28.

Referring to Table 22, MVDE approach is able to choose the optimal location and size of WTs units operating at the optimum power factor with a significant saving of power losses, and improvement of voltage profile enhancement than studied PSO, GA-PSO, ABC-CSO and ABC-BAT algorithms.

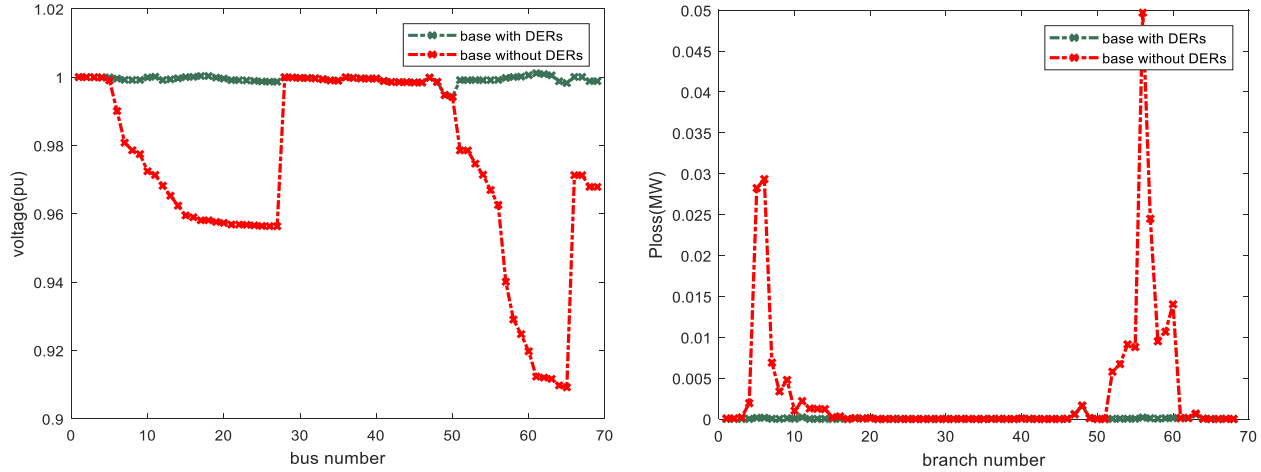

(a) Voltage profile (b) Power loss

Fig 28. System performance under annual load growth with integration DERs for base year (y=0)

Table.21 Simulation results for y=0

Case #		WT size MW, (location (bus no))/ PF	P_{loss} KW	Q_{loss} KVA	VD (PU)	V_{min} (location)	E_grid (Ib/h)
19	Without DERs	-	225	102.2		0.9092(65)	8245.7
	With DERs	1.7547(61)/0.85 0.50986(11)/0.85 0.38986(18)/0.85	4.98	7.07	0.0001	0.99426(50)	2359.7363

Table.22 Performance comparison for IEEE 69 bus radial distribution system with multiple WTs units

algorithms	WT size MW, (location (bus no))/ PF	P_{loss} KW	V_{min} (location)
MVDE	1.2094(30)/0.85 0.7502(13)/0.8669 1.0025(24)/0.8587	14.4	0.99289(8)
PSO [38]	2.293/0.81(61)	24.00	-
GA-PSO [36]	1425.7(30)/0.866 639.6(13)/0.866 168.4(10)/0.866	37.08	0.9712
ABC-CSO [36]	1394.1(30)/0.866 553.1(13)/0.866 296.8(10)/0.866	36.61	0.9763
ABC-BAT [36]	1336.2(30)/0.866 465.9(13)/0.866 201.2(10)/0.866	34.43	0.9798

b) Case 20 (y = 1)

The annual growth of load demand at the first year is presented in this case. From optimization results in Table 23, It is clear that the minimum voltage reduced from 0.9092(65) p.u at the base year to 0.9016 (56) p.u, after integrating WTs units this value increased to 0.99383(50) p.u, power loss and grid emission are reduced to 5.76 KW and 2532.7471 Ib/h, respectively. The power losses were decreased to 5.76 KW using the suggested strategy, in contrast to other algorithms. Fig 29(a) and Fig. 29(b) depict the voltage profile at each bus and the power loss at each bus, respectively.

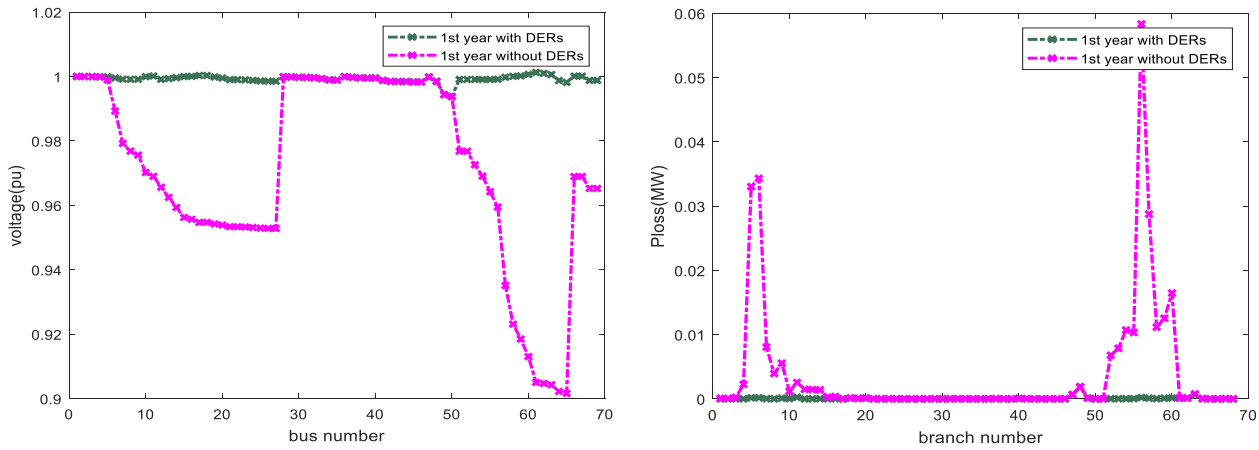

(a) Voltage profile (b) Power loss

Fig 29. System performance under annual load growth with integration DERs for first year (y=1)

Table.23 The best simulation results after WTs units' allocation at y=1

Case #		WT size MW, (location (bus no))/ PF	P_{loss} KW	Q_{loss} KVA	VD (PU)	V_{min} (location)	E_grid (Ib/h)
20	Without DERs	-	263.7	119.6		0.9016 (56)	8908.8
	MVDE	1.8852(61)/0.85 0.55451(11)/0.85 0.41622(18)/0.85	5.76	8.17	0.00012	0.99383(50)	2532.7471
	MOALO [39]	2(61)/0.8, 0.721(17)/0.83	11.259	-	-	0.98605(65)	-

c) Case 21 (y = 2)

This case displays the annual growth in system load demand through the second year (y=2). The performance of network at y=2 is found in Table 24, from the optimization result, the bus voltages are reduced below the minimum allowable limits (Vmin = 0.8933 p.u at bus 25), Inclusion of DERs is important for increasing minimum voltage to 0.99336 p.u at bus 50 upper the minimum allowable limits. The power loss is reduced by 97.848 %. The voltage profile at each bus and the power loss at each bus under the annual growth in system load demand during the second year are illustrated in Fig 30(a) and Fig. 30(b), respectively, it is observed that the MVDE algorithm has a great effect in reducing power loss and improving the voltage profile.

Table.24 Optimal WTs allocation in the 69-bus system (case 21)

Case #		WT size MW, (location (bus no))/ PF	P_{loss} KW	Q_{loss} KVA	VD (PU)	V_{min} (location)	E_grid (Ib/h)
21	Without DERs	-	309.5	140.3		0.8933 (225)	9630.3
	MVDE	2.0271(61)/0.85 0.44768(18)/0.85 0.59621 (11)/0.85	6.66	9.45	0.00014	0.99336 (50)	2721.8442

MOALO [39]	61(2.156(61)/0.8 17(0.775(17)/0.83	12.896	-	-	0.98522(65)	-

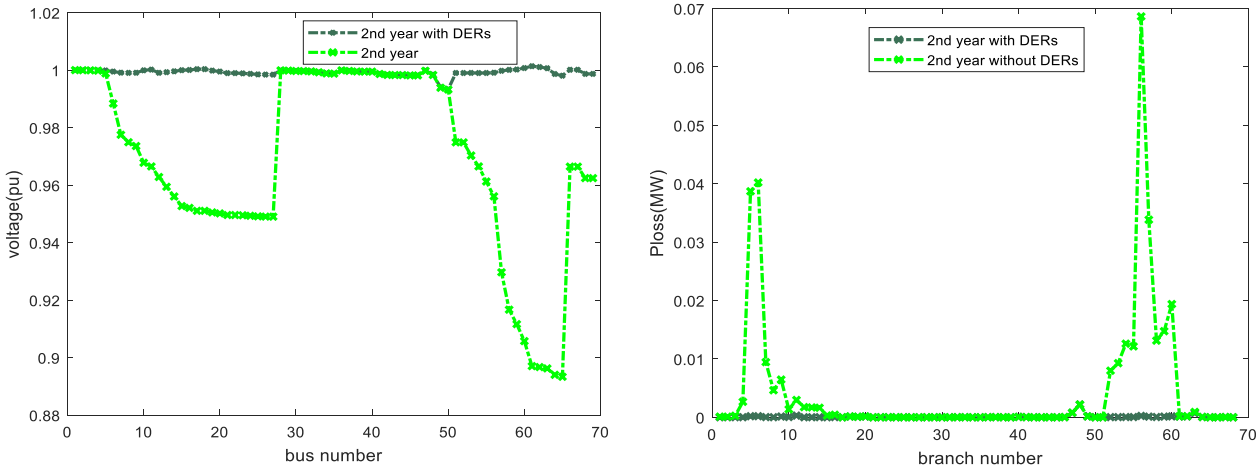

(a) Voltage profile (b) Power loss

Fig 30. System performance under annual load growth with integration DERs for second year (y=2)

d) Case 22 (y = 3)

MVDE method is presented to find the best allocation of three units of WTs units based on third years (y=3). The optimization results obtained from the optimization algorithm are tabulated in Table 25, it's evident that the total power loss and emission are decreasing and the WTs unit sizes are increasing due to annual growth in network load demand during the third year.

In order to study the feasibility of the proposed method, the voltage at each bus and power loss at each branch after using WT units with suitable size and location are shown in Fig. 31(a) and Fig. 31(b), obviously, the MVDE method achieves a good performance to improve the voltage profile and reduce power loss.

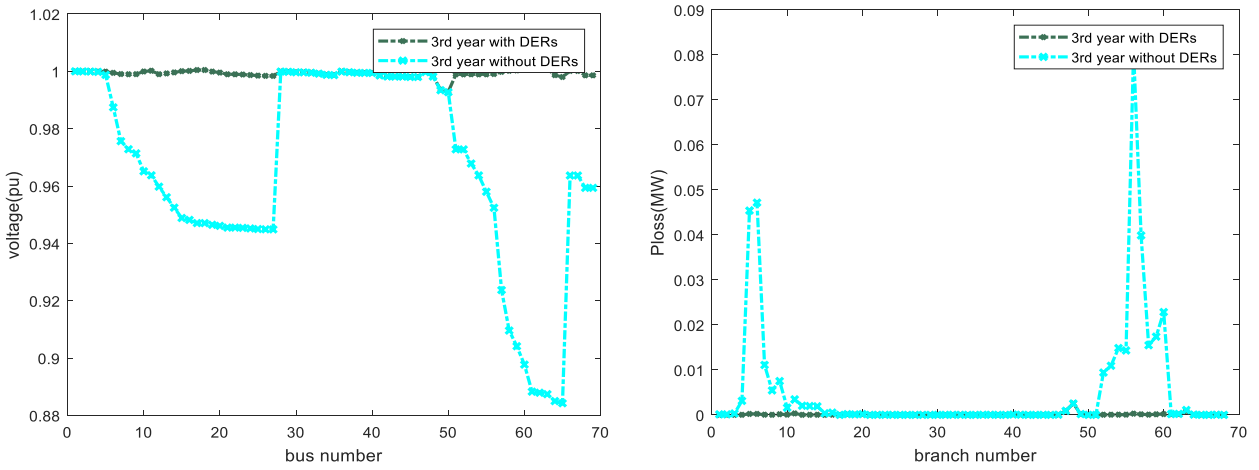

(a) Voltage profile (b) Power loss

Fig 31. System performance under annual load growth with integration DERs for third year (y=3)

Table.25 Simultaneous WTs allocation for evaluating environmental, and technical benefits at y=3

Case #		WT size MW, (location (bus no))/ PF	P_{loss} KW	Q_{loss} KVA	VD (PU)	V_{min} (location)	E_grid (Ib/h)
22	Without DERs	-	363.9	164.8		0.8842 (65)	10416
	MVDE	2.1819(61)/0.85 0.48377(18)/0.85001 0.63763(11)/0.85	7.7	10.92	0.00016	0.99286 (50)	2922.9708
	MOALO [39]	2.343(61)/0.8 0.830(17)/0.83	14.369	-	-	0.98500(65)	-

e) Case 23 (y = 4)

This case illustrates the annual growth of load demand at fourth year. From optimization results in Table 26, It is clear that the minimum voltage increased from 0.8743 (65) p.u to 0.99232 (50) p.u, after integrating three units of WTs, power loss and grid emission are reduced to 8.9 KW and 3138.1771 Ib/h, respectively. The results show that the MVDE algorithm performs better than the MOALO algorithm in terms of controlling power losses and enhancing the voltage profile.

The power loss at each bus and the voltage profile at each bus are visualized in Fig 32(a) and Fig. 32(b), respectively.

Table.1 Optimization results obtained at y=4

Case #		WT size MW, (location (bus no))/ PF	P_{loss} KW	Q_{loss} KVA	VD (PU)	V_{min} (location)	E_grid (Ib/h)
23	Without DERs	-	428.7	197		0.8743 (65)	11274
	MVDE	2.3454(30)/0.85 0.53161(18)/0.85 0.67668(11)/0.85	8.9	12.63	0.00018	0.99232 (50)	3138.1771
	MOALO [39]	2.556(61)/0.8 0.887(17)/0.83	15.859	-	-	0.98516(65)	-

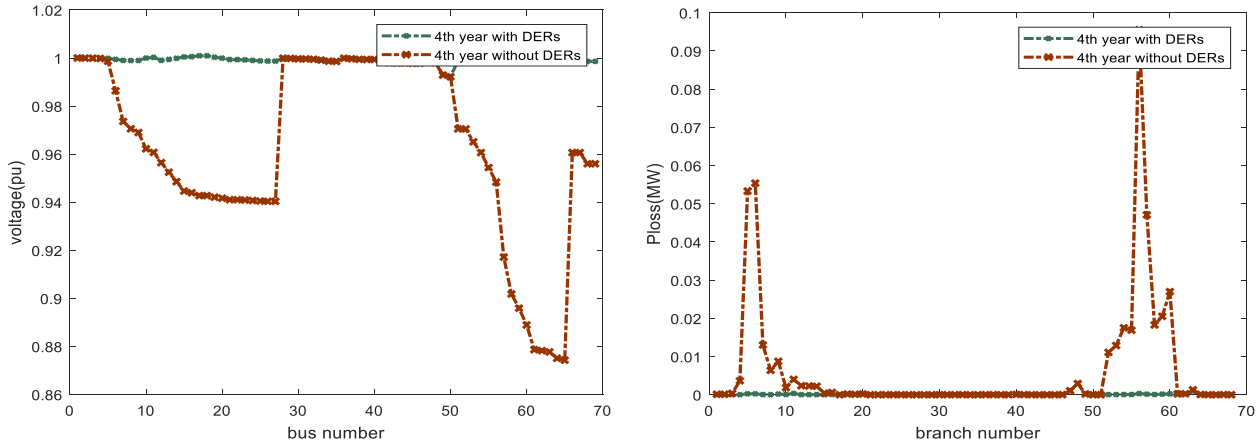

(a) Voltage profile (b) Power loss

Fig 32. System performance under annual load growth with integration DERs for fourth year (y=4)

f) Case 24 (y = 5)

In this case, the optimal optimization results are obtained for the fifth year (5th year), the voltage profile and the loss of the network are shown in Fig 33(a) and Fig. 33(b), respectively. The performance of the system is listed in table 27, it is evident that the MVDE algorithm reduces power losses and voltage variation better than the MOALO method, the power loss is reduced from 506.2 KW to 10.28 KW, the minimum voltage is increased to 0.99174 (50) p.u. The total emissions are reduced from 12213 Ib/h to 3368.9948Ib/h.

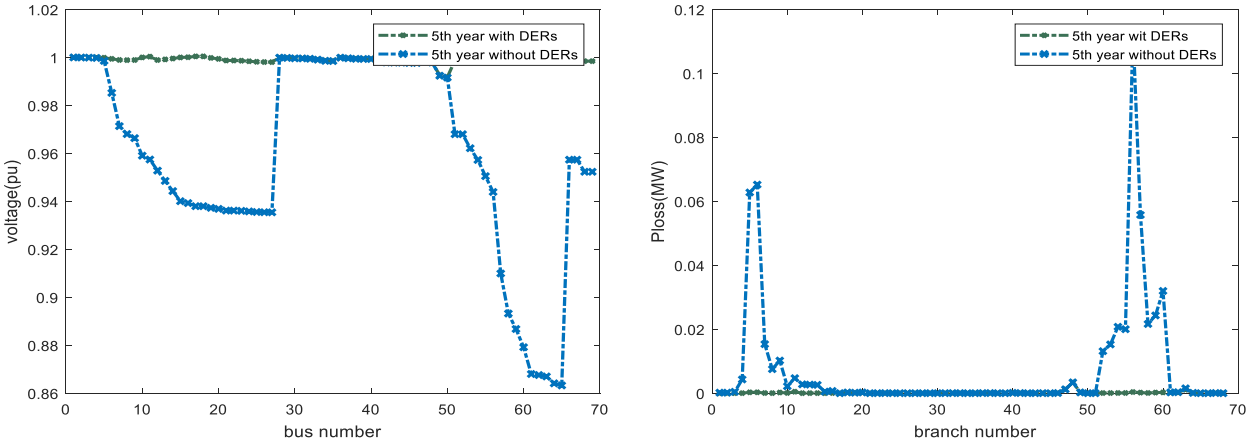

(a) Voltage profile (b) Power loss

Fig 33. System performance under annual load growth with integration DERs for fifth year (y=5)

Table.2 The best solutions obtained at y=5

Case #		WT size MW, (location (bus no))/ PF	P_{loss} KW	Q_{loss} KVA	VD (PU)	V_{min} (location)	E_grid (Ib/h)
24	Without DERs	-	506.2	228.7		0.8632 (65)	12213
	MVDE	2.5212(61)/0.85 0.55367(18)/0.85 0.74823(11)/0.8504	10.28	14.61	0.00021	0.99174 (50)	3368.9948

MOALO [39]	2.812(61)/0.8 0.944(17)/0.83	17.131	-	-	0.98630(65)	-

7. Conclusions

In this study, Multi-Variant Differential Evolution (MVDE) method is introduced to obtain the optimal allocation of different type of DERs like PV, WT, MT, and FC in radial distribution networks considering load growth up to planning period. The proposed paradigm has been applied on IEEE 33-bus, and IEEE 69-bus radial distribution system

In order to make the analysis more reliable, The Point Estimate Method (PEM) is used to model the stochastic behavior of the renewable power generation including PV and WT. Robust Optimization (RO) is applied for modeling the load uncertainty formulated by Gaussian distribution. From the optimization results, it is clear that

- The objective functions and size of DERs are changed with the load growth up to planning period and type of RES units considering probabilistic energy management.
- The overall impact of integrating renewable energy sources on technical, economic, and environmental benefits of the network with load growth is positive and proportionate.
- In addition, DERs from WT type given better results than DERs from PV type in terms of reduction power loss, and cost while improving voltage profiles.
- The optimal WTs size obtained are increased as compared to PVs size; whereas, PV type covered a wider portion of decision maker preferences.
- The proposed paradigm is effective for loss reduction in single objective, especially with increasing the system size.
  - For 33 bus system
- at y=0, the power loss is reduced by 64.721%, the minimum voltage increased to 0.96867 (33) p.u after using the PV distribution generator, and these results are improved to 14.42 KW and 0.99289 (8) p.u. respectively respectively after the integration of the WT generating system.
- After first year, with using PV units, the minimum voltage has been increased from 0.9059(18) p.u to 0.96628(33) p.u. The losses were decreased to 83.02 KW. with using WT units The total losses reduced to 16.64 MW The minimum voltage increased to 0.99242 p.u
- considering y=2 and PV DGs types The power loss reduced by 65.28 % .The emissions reduced to 7112.4424 Ib/h , these value was improved after using DGs from WT type.
- After three years from planning and integrating PV units, the total power loss and emission are decreasing to 122 KW and 7659.5978 Ib/h.
- The power losses were reduced by 34 %, and voltage deviation was reduced to 0.02439 p.u in fourth year under planning for the PV power generation system. after planning the WT types these results were changed to 0.99073 p.u minimum voltage, and 25.75 KW power loss,
- At the fifth year, the best optimization results were obtained after using WT units where the power loss was reduced from 449.5 KW to 29.79 KW, the minimum voltage deviation was increased to 0.99017 p.u.
  - Under the planning of hybrid power system model to reduce power loss the cost and

emissions

- in base year, the sizes of PV and WT units must be equal to 171.3, 143, 59.31, and 57.05, respectively.
- At y=1, The sizes of PV and WT units are increased to146.8, 173.2, 59.2, and 63.93 KW, respectively.
- at second year, the sizes of PV and WT units are 140.6, 155.2, 60.32, and 60.13 KW, respectively. large sizes of PV 2 and the small sizes of PV 1 leads to minimize power losses and WT sizes are in the range [0.056 - 0.07] MW.
- the sizes of PV 1 and WT 2 are large, and the sizes of PV 2 and WT 1 are small at y=3.
- The sizes of PV and WT units are changed from 171.3, 143, 59.31, and 57.05 KW at base case (y=0) to 144.7, 144, 52.72, and 57.33 KW at fourth year (y=4), respectively.
- At fifth year, The PV and WT sizes are 156.6, 130.1, 61.08, and 62.53 KW, respectively, leads to improve the system performance.
    - For 69 bus system
- the total capacity of each unit of DERs increases due to increase in the load demand through five years

References

[1] Faraji, J., Hashemi-Dezaki, H., & Ketabi, A. (2020). Multi-year load growth-based optimal planning of grid-connected microgrid considering long-term load demand forecasting: A case study of Tehran, Iran. *Sustainable Energy Technologies and Assessments*, *42*, 100827.

[2] Kazmi, S. A. A., Ameer Khan, U., Ahmad, H. W., Ali, S., & Shin, D. R. (2020). A Techno-Economic Centric Integrated Decision-Making Planning Approach for Optimal Assets Placement in Meshed Distribution Network Across the Load Growth. *Energies*, *13*(6), 1444.

[3] Bizon, N., Lopez-Guede, J. M., Kurt, E., Thounthong, P., Mazare, A. G., Ionescu, L. M., & Iana, G. (2019). Hydrogen economy of the fuel cell hybrid power system optimized by air flow control to mitigate the effect of the uncertainty about available renewable power and load dynamics. *Energy Conversion and Management*, *179*, 152-165.

[4] Yang, Y., Yu, J., Yang, M., Ren, P., Yang, Z., & Wang, G. (2019). Probabilistic modeling of renewable energy source based on Spark platform with large-scale sample data. *International Transactions on Electrical Energy Systems*, *29*(3), e2759.

[5] Jithendranath, J., & Das, D. (2019). Scenario-based multi-objective optimisation with loadability in islanded microgrids considering load and renewable generation uncertainties. IET Renewable Power Generation, 13(5), 785-800.

[6] Saleh, A. A., Senjyu, T., Alkhalaf, S., Alotaibi, M. A., & Hemeida, A. M. (2020). Water cycle algorithm for probabilistic planning of renewable energy resource, considering different load models. *Energies*, *13*(21), 5800.

[7] Mohamed, A. A. A., Ali, S., Alkhalaf, S., Senjyu, T., & Hemeida, A. M. (2019). Optimal Allocation of Hybrid Renewable Energy System by Multi-Objective Water Cycle Algorithm. *Sustainability*, *11*(23), 6550.

[8] Hemeida, A. M., El-Ahmar, M. H., El-Sayed, A. M., Hasanien, H. M., Alkhalaf, S., Esmail, M. F. C., & Senjyu, T. (2020). Optimum design of hybrid wind/PV energy system for remote area. *Ain Shams Engineering Journal*, 11(1), 11-23.

[9] Alavi, S. A., Ahmadian, A., & Aliakbar-Golkar, M. (2015). Optimal probabilistic energy management in a typical micro-grid based-on robust optimization and point estimate method. *Energy Conversion and Management*, *95*, 314-325.

[10] Hemeida, M. G., Alkhalaf, S., Mohamed, A. A. A., Ibrahim, A. A., & Senjyu, T. (2020). Distributed Generators Optimization Based on Multi-Objective Functions Using Manta Rays Foraging Optimization Algorithm (MRFO). *Energies*, *13*(15), 3847.

[11] Rueda-Medina AC, Franco JF, Rider MJ, Padilha-Feltrin A, Romero R (2013) A mixed integer linear programming approach for optimal type, size and allocation of distributed generation in radial distribution systems. *Electr Power Syst Res* 97:133–143.

[12] Remha S, Saliha C (2018) A novel multi-objective bat algorithm for optimal placement and sizing of distributed generation in radial distributed systems. *Adv Electr Electron Eng* 15:736–746

[13] Ferraz, R. S., Ferraz, R. S., & Rueda–Medina, A. C. (2023). Multi-objective Optimization Approach for Allocation and Sizing of Distributed Energy Resources Preserving the Protection Scheme in Distribution Networks. *Journal of Control, Automation and Electrical Systems*, *34*(5), 1080-1092.

[14] Pham, T. D., Nguyen, T. T., & Dinh, B. H. (2020). Find optimal capacity and location of distributed generation units in radial distribution networks by using enhanced coyote optimization algorithm. *Neural Computing and Applications*, 1-29.

[15] Alkhalaf, S., Senjyu, T., Saleh, A. A., Hemeida, A. M., & Mohamed, A. A. A. (2019). A MODA and MODE comparison for optimal allocation of distributed generations with different load levels. *Sustainability*, *11*(19), 5323.

[16] Alsadi, S., & Khatib, T. (2018). Photovoltaic power systems optimization research status: A review of criteria, constrains, models, techniques, and software tools. *Applied Sciences*, *8*(10), 1761.

[17] Yang, B., Guo, Y., Xiao, X., & Tian, P. (2020). Bi-level capacity planning of wind-PV-battery hybrid generation system considering return on investment. *Energies*, *13*(12), 3046.

[18] Gamil, M. M., Sugimura, M., Nakadomari, A., Senjyu, T., Howlader, H. O. R., Takahashi, H., & Hemeida, A. M. (2020). Optimal sizing of a real remote Japanese microgrid with sea water electrolysis plant under time-based demand response programs. *Energies*, *13*(14), 3666.

[19] Susowake, Y., Masrur, H., Yabiku, T., Senjyu, T., Motin Howlader, A., Abdel-Akher, M., & M. Hemeida, A. (2019). A multi-objective optimization approach towards a proposed smart apartment with demand-response in Japan. *Energies*, *13*(1), 127.

[20] Zishan, F., Mansouri, S., Abdollahpour, F., Grisales-Noreña, L. F., & Montoya, O. D. (2023). Allocation of Renewable Energy Resources in Distribution Systems while Considering the Uncertainty of Wind and Solar Resources via the Multi-Objective Salp Swarm Algorithm. Energies, 16(1), 474

[21] Yang, M., Cui, Y., & Wang, J. (2023). Multi-Objective optimal scheduling of island microgrids considering the uncertainty of renewable energy output. International Journal of Electrical Power & Energy Systems, 144, 108619.

[22] Hadi Abdulwahid, A., Al-Razgan, M., Fakhruldeen, H. F., Churampi Arellano, M. T., Mrzljak, V., Arabi Nowdeh, S., & Moghaddam, M. J. H. (2023). Stochastic multi-objective scheduling of a hybrid system in a distribution network using a mathematical optimization algorithm considering generation and demand uncertainties. Mathematics, 11(18), 3962.

[23] Liu, Z., Cui, Y., Wang, J., Yue, C., Agbodjan, Y. S., & Yang, Y. (2022). Multi-objective optimization of multi-energy complementary integrated energy systems considering load prediction and renewable energy production uncertainties. Energy, 254, 124399.

[24] Mohammed, N. A., & Al-Bazi, A. (2022). An adaptive backpropagation algorithm for long-term electricity load forecasting. Neural Computing and Applications, 34(1), 477-491.

[25] Naghdi, M., Shafiyi, M. A., & Haghifam, M. R. (2019). A combined probabilistic modeling of

renewable generation and system load types to determine allowable DG penetration level in distribution networks. International Transactions on Electrical Energy Systems, 29(1), e2696.

[26] Malik, M. Z., Kumar, M., Soomro, A. M., Baloch, M. H., Farhan, M., Gul, M., & Kaloi, G. S. (2020). Strategic planning of renewable distributed generation in radial distribution system using advanced MOPSO method. Energy Reports, 6, 2872-2886.

[27] Ali, A., Abbas, G., Keerio, M. U., Mirsaeidi, S., Alshahr, S., & Alshahir, A. (2023). Multi-objective optimal siting and sizing of distributed generators and shunt capacitors considering the effect of voltage-dependent nonlinear load models. IEEE Access, 11, 21465-21487.

[28] Ali, M. H., Kamel, S., Hassan, M. H., Tostado-Véliz, M., & Zawbaa, H. M. (2022). An improved wild horse optimization algorithm for reliability based optimal DG planning of radial distribution networks. *Energy Reports*, *8*, 582-604.

[29] Hadi Abdulwahid, A., Al-Razgan, M., Fakhruldeen, H. F., Churampi Arellano, M. T., Mrzljak, V., Arabi Nowdeh, S., & Moghaddam, M. J. H. (2023). Stochastic multi-objective scheduling of a hybrid system in a distribution network using a mathematical optimization algorithm considering generation and demand uncertainties. Mathematics, 11(18), 3962.

[30] Jayaram, K., Ravindra, K., Prasad, K. R. K. V., & Murthy, K. R. (2022). A multi-objective approach for renewable distributed generator unit's placement considering generation and load uncertainties. International Journal of Energy and Environmental Engineering, 1-25.

[31] Zishan, F., Mansouri, S., Abdollahpour, F., Grisales-Noreña, L. F., & Montoya, O. D. (2023). Allocation of Renewable Energy Resources in Distribution Systems while Considering the Uncertainty of Wind and Solar Resources via the Multi-Objective Salp Swarm Algorithm. Energies, 16(1), 474.

[32] Wang, S., Wang, K., Teng, F., Strbac, G., & Wu, L. (2018). An affine arithmetic-based multi-objective optimization method for energy storage systems operating in active distribution networks with uncertainties. Applied Energy, 223, 215-228.

[33] Ramadan, A., Ebeed, M., Kamel, S., Abdelaziz, A. Y., & Haes Alhelou, H. (2021). Scenario-based stochastic framework for optimal planning of distribution systems including renewable-based dg units. Sustainability, 13(6), 3566.

[34] Naghdi, M., Shafiyi, M. A., & Haghifam, M. R. (2019). A combined probabilistic modeling of renewable generation and system load types to determine allowable DG penetration level in distribution networks. International Transactions on Electrical Energy Systems, 29(1), e2696.

[35] Taghikhani, M. A. (2021). Renewable resources and storage systems stochastic multi-objective optimal energy scheduling considering load and generation uncertainties. Journal of Energy Storage, 43, 103293.

[36] Palanisamy, R., & Muthusamy, S. K. (2020). Optimal Siting and Sizing of Multiple Distributed Generation Units in Radial Distribution System Using Ant Lion Optimization Algorithm. *Journal of Electrical Engineering & Technology*, 1-11.

[37] Ayanlade, S. O., Ariyo, F. K., Jimoh, A., Akindeji, K. T., Adetunji, A. O., Ogunwole, E. I., & Owolabi, D. E. (2023). Optimal allocation of photovoltaic distributed generations in radial distribution networks. *Sustainability*, *15*(18), 13933.

[38] Parihar, S. S., & Malik, N. (2020). Optimal allocation of renewable DGs in a radial distribution system based on new voltage stability index. *International Transactions on Electrical Energy Systems*, *30*(4), e12295.

[39] Abdel-mawgoud, H., Kamel, S., Ebeed, M., & Youssef, A. R. (2017, December). Optimal allocation of renewable dg sources in distribution networks considering load growth. In *2017 Nineteenth International Middle East Power Systems Conference (MEPCON)* (pp. 1236-1241). IEEE.

[40] Abdel-mawgoud, H., Kamel, S., Ebeed, M., & Youssef, A. R. (2017, December). Optimal allocation of renewable dg sources in distribution networks considering load growth. In *2017 Nineteenth International Middle East Power Systems Conference (MEPCON)* (pp. 1236-1241). IEEE.

[41] Esmaeili M, Sedighizadeh M, Esmaili M. Multi-objective optimal reconfiguration and DG (Distributed Generation) power allocation in distribution networks using Big Bang-Big Crunch algorithm considering load uncertainty. *Energy*, 2016; *103*: 86-99.

[42] Kefayat M, Ara AL, Niaki SN. A hybrid of ant colony optimization and artificial bee colony algorithm for probabilistic optimal placement and sizing of distributed energy resources. *Energy Conversion and Management*, 2015; *92*: 149-161.149-161.

[43] Aghajani, G. R., Shayanfar, H. A., & Shayeghi, H. (2017). Demand side management in a smart micro-grid in the presence of renewable generation and demand response. *Energy*, *126*, 622-637.

[44] Moradi, M. H., Eskandari, M., & Hosseinian, S. M. (2014). Operational strategy optimization in an optimal sized smart microgrid. *IEEE Transactions on Smart Grid*, *6*(3), 1087-1095.

[45] Kefayat M, Ara AL, Niaki SN. A hybrid of ant colony optimization and artificial bee colony algorithm for probabilistic optimal placement and sizing of distributed energy resources. Energy Convers Manage. 2015; 92:149-161.

[46] Alavi SA, Ahmadian A, Aliakbar-Golkar M. Optimal probabilistic energy management in a typical micro-grid based-on robust optimization and point estimate method. Energy Convers Manage. 2015; 95:314-325.

[47] Boursianis, A. D., Papadopoulou, M. S., Nikolaidis, S., Sarigiannidis, P., Psannis, K., Georgiadis, A, & Goudos, S. K. (2021). Novel design framework for dual-band frequency selective surfaces using multi-variant differential evolution. *Mathematics*, *9*(19), 2381.

[48] Hassan, S., Hemeida, A. M., Alkhalaf, S., Mohamed, A. A., & Senjyu, T. (2020). Multi-variant differential evolution algorithm for feature selection. Scientific Reports, 10(1), 17261.

[49] Sahoo NC, Prasad K (2006) A fuzzy genetic approach for network reconfiguration to enhance voltage stability in radial distribution systems. Energy Convers Manag 47(18–19):3288–3306

[50] Saleh, A. A., Mohamed, A. A. A., & Hemeida, A. M. (2019, February). Impact of Optimum Allocation of Distributed Generations on Distribution Networks Based on Multi-Objective Different Optimization Techniques. In 2019 International Conference on Innovative Trends in Computer Engineering (ITCE) (pp. 401-407). IEEE.

[51] Pham, T. D., Nguyen, T. T., & Dinh, B. H. (2020). Find optimal capacity and location of distributed generation units in radial distribution networks by using enhanced coyote optimization algorithm. *Neural Computing and Applications*, 1-29.

[52] Savier, J. S., & Das, D. (2007). Impact of network reconfiguration on loss allocation of radial distribution systems. IEEE Transactions on Power Delivery, 22(4), 2473-2480.

NOMENCLATURE			
A_c	Surface areas of the arrays (m2)	P_{gnj}	Active power generated by DG at bus n_j
$AP_{DERs,k}$,	the active of the kth DERs	P_{gnj}^{min}	The upper limit of the real power delivered by new electric units at bus nj
AP_{Gr}	*the* active powers that is taken from grid.	P_{gnj}^{max}	The lower limit of the real power delivered by new electric units at bus nj
$AP_{Lo,i}$	the active powers at the ith load.	P_{grid}	Active power from the main substation
β_w	Shape parameter	p_{loss}	Active power losses
$C_{cap,i}$	The capital cost of DG	$P_{pv}(s_i)$	Power produced from Photovoltaic system (kW) for the amount of irradiance s
$C_{F,i}$	Cost of fuel for DG	P_{wt}	Power produced from WT
C_{FC}	Fuel consumption expenses in FCs ($/h).	p_R	Rated power of the turbine = 15 KW.
C_{gasFC}	Natural gas price feeding the FC	PVS	Photovoltaic system
C_{gasMT}	Natural gas price feeding the MT	Q_{dnj}	Reactive load power at bus n_j
C_{MT}	Fuel consumption expenses in MT ($/h).	Q_{gnj}^{min}	The upper limit of the imaginary power delivered by new electric units at bus n_j
$C_{O\&M,i}$	DES operation & maintenance cost	Q_{gnj}	Imaginary power delivered by new electric units at bus n_j
$Cost_{DERs,i}^{FX}$	The initial cost of DES	Q_{gnj}^{max}	The lower limit of the imaginary power delivered by new electric units at bus nj
$Cost_{DERs,i}$	The cost of DES connected in bus i	Q_{loss}	Reactive power losses
$cost_{grid}$	The cost at which energy was purchased from the main substation	$Q_L(0)$	The initial reactive power loads
DERs	Distributed energy resource	$Q_L(y)$	The reactive power load at y year
d_{max}^i	controls the search intensity near the sea	Q_i	The reactive powers flow from buses i to bus i + 1
FC	Full cell unit	r_J	The resistance of the branch J
E_{MTi}	Emission produced from MT	RDN	Radial distribution network

E_{FCi}	Emission produced from FC	$RP_{DERs,k}$	*The* reactive powers of the kth DERs
E_{WTi}	Emission produced from WT	$RP_{Lo,i}$	The reactive powers at the ith load.
E_{PVi}	Emission produced from PV	RP_{Gr}	The reactive powers that is taken from grid.
E_{Grid}	Emission produced from main substation	rb	The annual rate of benefit
g	The annual growth rate of system loads	s_i	Solar irradiance (kW/m2)
$K_{DES,i}$	DES i Capacity Factor	SO	Single objective
LB	lower bounds defined by the given problem	$TAPL_{DERs}$	*The* total active power losses of the System after integrating DERs
MOWC	Multi Objective Water cycle	$TAPL_{DERs}$	The total reactive power losses of the
A	Algorithm		system after integrating DERs
MO	Multi-objective	t	Number of current iteration
MT	Micro turbine	T	DG life time
n_{bus}	Total number of buses	V_i^{min}	Minimum voltage of bus i
n_{br}	Total number of branches.	V_i^{max}	Maximum voltage of bus i
N_{DES}	Total number of new electrical units	v_{ci}	Cut-in wind turbine speed
N_{MT}	Total number of MT	v_{co}	Cut-off wind turbine speed = 18 m/s
N_{FC}	Total number of FC	V_m	Average wind speed for a specific location
N_{WT}	Total number of WT	V_i	The voltage magnitudes of bus i
N_{PV}	Total number of PV	V_{i+1}	the voltage magnitudes of bus i + 1
Npop	Number of population	v_r	Appraised speed of the wind turbine = 3.5m/s
N_{sr}	The summation of number of rivers	V_{wind}	Actual wind turbine speed =17.5 m/s
Ns_n	The number of streams which flow to the specific rivers and sea.	$rand$	An uniformly distributed random number between0 and 1
$P_{cap,i}$	DG capacity	x_J	*the* reactance of the branch J
P_{dnj}	Active load power at bus n_j	Y_{nj}	Admittance between bus n_i and bus m_i
$P_{DERs,i}$	The real power offered by the new electrical units at bus n_i	y	The number of year
P_{FC}	Power produced from FC	η	Efficiency of the PV system
$P_L(y)$	The active and reactive power load at y year	η_{MT}	Efficiency of MT
$P_L(0)$	The initial active power loads	η_{FC}	Efficiency of FC
P_i	The active powers flow from buses i to bus i + 1	δ_{mj}	Phase angle of voltage at bus m_j
P_{MT}	Power produced from MT	δ_{nj}	Phase angle of voltage at bus n_j
π_{grid}	Energy price from the main substation	θ_{nj}	Phase angle of Y_j